Planar Discontinuity Modeling in 3D Space by Application of Reciprocity Theorem Combined with MGEC

Raja Mchaalia

République Tunisienne
Ministère de l'Enseignement Supérieur et de la Recherche Scientifique
Université de Tunis El Manar
Ecole Nationale d'Ingénieurs de Tunis

THESIS

In order to obtain
DOCTORATE OF THE UNIVERSITY TUNIS EL MANAR

Issued by:
National Engineering School of Tunis

Specialty:
Communications Systems

Presented and Supported by:
Raja Mchaalia
In: July 20th, 2019

Subject

Planar Discontinuity Modeling in 3D Space by Application of Reciprocity Theorem Combined with MGEC

Jury

President	: Mr. Ammar Bouallègue, Professor, ENIT
Reviewers	: Mr. Ridha Bouallègue, Professor, SUPCOM : Mr. Jamel BelHadj Tahar, Professor, ENISO
Examiner	: Mr. Faouzi Bahloul, Lecturer, ENIT
Supervisor	: Mr. Taoufik Aguili, Professor, ENIT

Doctoral School :
Engineering Sciences and Technology

Research Laboratory:
Communication Systems

B.P. 37. 1002 Le Belvédère Tunis. Tunisie ص ب 37. البلفدار تونس 1002. تونس
Tél. : +216 70 014 400 الهاتف : Fax : +216 71 872 729 / +216 70 860 548 الفاكس : www.enit.rnu.tn

Thesis is Communication, Discussion, Team Working and Continuity.

Raja Mchaalia

Don't Believe in Luck.
Believe in Hard Work

To my Mum soul that i wished to be with me in this special day,
To my beautiful Dad,
To my Brothers and Sisters,
To my nieces and nephews especially my lovers Elyes and Edriss,
To my Family,
To my cute indian friend Gopi Krishna who supported, advised and encouraged me all the time,
To all my Syscom Laboratory friends especially Lovely Hafewa, Mohamed Bedoui, Kaouther, Auns, Ines, Nabiha, Wided, Zied BelHadj Alaya,..,
To my other friends inside and outside tunisia.

Acknowledgment

I would like to express my deepest thanks and gratitude to my supervisor Professor **Taoufik Aguili** for his continuous support, Kindness, patience, motivation, and immense knowledge. His precious guidance and fruitful ideas helped me in all the time of research and writing of my scientific papers as well as this manuscript. His valuable advices, enthusiasm and constant support during this thesis allowed me to acquire new understandings and extend my experiences. I am thankful for the opportunities he provided, and for having faith in me. I deeply hope that we can continue our collaboration.

I would like to thank all members of the jury. I thank Professor **Ammar Boullague** for accepting being my president thesis. I thank Professor **Ridha Bouallegue** and Professor **Jamel BelHadj Tahar** for accepting being my thesis reviewers and for their insightful comments and encouragement. I also thank Professor **Faouzi Bahloul** for accepting being my thesis examiners.

A special gratitude is also due to our colleague Professor **Fethi Mejri** for his great advices and his guidance.

A Special thanks to my colleague and my friend **Mourad Aidi** for the beneficial collaboration we have had. I am deeply grateful for the great deal of time we spent discussing many technical details of my work together.

Raja Mchaalia

Abstract

The 3D planar discontinuity presents several difficulties related to the volume mesh. The entire volume space must be taken into account even the smallest details. In this thesis, we propose a formulation based on the Reciprocity Theorem combined with the Generalized Equivalent Circuit Method (MGEC) to model a planar discontinuity of RF circuits which excited by a coaxial cable. The major advantage of this formulation is the fact to reduce the computational volume into a 2D ones in the discontinuity plane. Also, we focused on the calculation of the discontinuity between the excitation source and the planar structure to determine the exact behavior of the electric coaxial excitation model. The obtained current density, electric field distributions, and the input impedance are presented and discussed in the following Sections. An approximately good agreement of input impedance with those obtained by the simulator and measurement is shown. The 3D concept of hybridization is also proved by the modeling of microstrip antenna which connected to the conductor and excited by coaxial cable. Results obtained in the current density of antenna shown the existing of the discontinuity between antenna and conductor. As well as a mathematical formulation based on hybridization to model a microstrip filter.
Keywords. Reciprocity Theorem, MGEC, Discontinuity, Modeling, Circuit Analyzing, localized source.

Resumé

Le calcul de la discontinuité dans l'espace 3D présente plusieurs difficultés qui liées au maillage volumique. En fait, tout l'espace du volume entier doit être pris en considération même pour les petits détails. Dans cette thèse, nous proposons une formulation basée sur le théorème de réciprocité combiné avec la méthode des circuits électriques généralisées (MGEC) pour modéliser des structures planaires ou fermées excité par deux sources (planaire et coaxiale). L'avantage majeur de cette formulation est le fait de réduire le calcul volumique en calcul surfacique dans le plan de discontinuity. De plus, nous nous sommes concentrés sur le calcul de la discontinuité entre l'excitation et la structure planaire dans le but de déterminer le circuit électrique de model coaxial. La densité du courant et le champ électrique distribués ainsi que l'impédance d'entrée sont présentés et discutés par la suite. Un accord approximatif de la valeur de l'impédance d'entrée avec celles obtenues par le simulateur et la mesure. Le concept de l'hybridation est aussi prouvé par la modélisation d'une antenne microstrip connecté à un conducteur et excitée par un câble coaxial dont sa valeur de la densité du courant montre l'existence d'une discontinuité entre l'élément rayonant et le conducteur. Ainsi que, une formlation mathématique basée sur l'hybridation de modéliser un filtre microstrip.

Mots Clés. Théorème de Réciprocité, MGEC, Discontinuité, Modelisation, Analyse de Circuit, source localisée.

Table of contents

List of Tables

List of Figures

Chapter 1

General Introduction

1.1 Context

Microwaves are a form of electromagnetic radiation[1], just like radio waves, ultraviolet rays, X-rays and gamma rays. They are of intermediate wavelength between infrared and broadcast waves, approximately in the range of 30 centimeters (1 GHz) to 1 millimeter (300 GHz). Microwaves cover the end of UHF (from 1 to 3 GHz), SHF (from 3 to 30 GHz) and EHF (from 30 to 300 GHz)[2–4]. Microwaves have interesting applications including those used for satellite transmissions (case of the GPS), mobile communications, broadcasting of terrestrial digital television programs, radar applications, medicine, industrial heating and even cooking food[5–9]. However, the advantages of the microwave can be resumed in those things:

- The microwave spectrum has larger bandwidth and a hence large amount of information can be transmitted using it.
- Microwave technology helps to manage crowded spectrum with the use of highly selective receivers, modulation (SSB, PSK, QAM, etc.) and spread spectrum techniques, data compression, etc.
- The microwave spectrum is divided into different channels as per application.
- The microwave communication is used since earlier days as one of the Line of Sight Communication in hilly remote areas where other means of wired communication is not possible to be installed.

It has also some disadvantages, among those:

- For the frequencies in the microwave range, E-H wave analysis needs to be applied.
- At microwave frequencies, the transit time of the current carrier i.e. electron is higher which takes a large percentage of the actual signal. Due to this fact, conventional transistors do not function properly at microwave frequency compare to lower frequency.
- As microwave communication is limited to line of sight mode only.

- As we know lumped components such as resistors, inductors and capacitors do not have the same characteristics at microwave frequencies as they have at lower frequencies

Thereof, with the increasing complexity of microwave integrated circuits, passive component modeling becomes more and more important in accurately determining the performance of the designed circuits[10, 11]. Also, Scientists and mathematicians of the nineteenth century laid the foundation of telecommunication and wireless technology, which has affected all facets of modern society. In 1864, James C. Maxwell[12] put forth fundamental relations of electromagnetic fields that not only summed up the research findings of Laplace, Poisson, Faraday, Gauss, and others[13] but also predicted the propagation of electrical signals through space[14]. Since Maxwell's equations involve vector differential or integral operations on vector field quantities, and these fields are functions of special coordinates[15].

1.2 Thesis objectives

Otherwise, a field theory solution generally provides a complete description of the electromagnetic field at every point in space, which usually gives much more information than we need for most practical purposes. Consequently, the problem of electromagnetic (EM) propagation in stratified isotropic and anisotropic media has been studied extensively[16]. However, this field is neither a purely TE nor a purely TM mode, rather it is a hybrid mode and cannot be obtained from a single scalar potential[17]. Besides, full-wave three-dimensional-discretization numerical methods are considered the most versatile, as they apply to geometrically more complex structures at higher frequencies. Just as the high frequencies and short wavelengths of microwave energy make for difficulties in the analysis and design of microwave devices and systems especially in space (3D dimensions). In the design of microwave of [18] microstrip and millimeter-wave circuits, compensation of microstrip discontinuities is widely used to reduce the effects of discontinuity reactance. For low-frequency applications, planar waveguide models have been successfully applied for compensation of some discontinuities such as steps, right-angle bends and T junctions. At higher frequencies and three-dimensional space, a dynamic model based on a full-wave analysis is required to take into account more physical effects such as radiation and surface-wave losses. Furthermore, it is necessary to take advantage of the ability to optimize analog and digital simultaneously to reach our goals. There are many algorithms and circuit techniques that have been employed at a high frequency that may bring benefits to the microwave space. For this reason, we resort obligatory for electromagnetic methods named "global methods". These methods can be classified into two groups: integral and differential[19]. Differential methods like the finite-difference time-domain (FDTD)[20] approach, the transmission-line matrix method (TLM)[21] and finite element method (FEM)[22]. These methods use a structured grid for spa-

tial discretization. However, they are quite costly in terms of their computational requirements. Integral methods also adapt well to these types of problems. Among the integral methods, we can cite the method of moment (MOM). The method of moment gives a general procedure for treating field problems, but the details of the solution vary widely with the particular problem. It is perhaps the most widely used tool for electromagnetic modeling. The advantages of the method of moment are accuracy, versatility, and the ability to compute near as well as as-far zone parameters. The most widely used forms of method of moment are the thin wire computer programs[23]. Despite its advantages, it has been proven its insufficiency when it comes to 3D problems[24, 25]. To remedy this drawback, we propose a hybridization of methods that combines the one mentioned before (MOM or a version of it named MGEC) with the reciprocity theorem(RT)[26]. Also, the reciprocity theorem is among the most useful tool in fields and circuit problems. Thereby, the principle of reciprocity was formulated and established some time ago. As we shall demonstrate, this principle proves to be a powerful tool of investigation, establishing a far-reaching analogy in the performance of receiving and transmitting antennas and after that for electromagnetic radiation structures[27]. It also has been used to study scattering, interference, ultra-wide-band and discontinuity problems existing in radiate planar structures. Basing on these approaches, we try in this work to concentrate on the study and the analysis of discontinuity phenomena existing between source and microwave circuit using hybridization. In this thesis, we apply and validate this latest technique by the meaning of reciprocity theorem combined with the EGC method to model planar structure which based on the microstrip resonator, microstrip antenna and developing the theoretical concept of a microstrip filter for 5G applications.

1.3 Thesis outline

Our manuscript is divided into five chapters as follows:
− The present chapter is an overview of microwaves, their applications, problems encountered in microwaves circuits and with which tools it can resolve. Also, it shows the content of other chapters − In the second chapter 2, we introduce the discontinuity problems existing in microwave components. We will also give an overview of the discontinuity problems existing between microwave structure elements as well as at the source. Furthermore, we will cite the different research which started this type of problem by concentrating on the discontinuity between source and planar structure .
− In the third chapter 3, we will apply the reciprocity theorem by developing its mathematical formulation giving the original expression of the excitation source which was the aim of our conference paper. To show the efficiency of this theorem, we will apply and validate it to our first example which described by a microstrip resonator in an open-end metallic waveguide excited by coaxial cable. For the first time, we will calculate the value of current and field distribution as mentioned in our conference paper. After that, we will give the value of input impedance given by the source and

compare it to HFSS and the one seen by the fundamental indicates the existence of discontinuity.
− In the fourth chapter 4, we will study this discontinuity, which was the aim of our journal paper, calculating its parameters and giving the equivalent electric discontinuity circuit and its parameter. As well as, we will give the relationship between planar and coaxial source parameters. Finally, we will give an example of a planar source applying the reciprocity theorem.
− In the last chapter 5, we will model microstrip antenna connected to the conductor and excited by coaxial source. We will show if conductor dimensions affect on current value and behavior. Another example will be modeled which defined by the microstrip filter for 5G applications using the hybridization to give its theoretical concept in transmitter parameter values.

Chapter 2

Introduction to Discontinuity Between Source and Circuit in 3D Space

Contents

2.1 Research Context

Wireless communications in the literature are very rich with analytical studies and measurement campaigns that study the nature of the wireless propagation waves. Despite their undoubted usefulness, many of these studies have omitted a fundamental yet key feature of the physical signal propagation[28]. However, signal propagation in wireless channels can be subjected to many types of environmental parameters that degrade its performance. Such factors include noise, discontinuity, interference,

large-scale fading, small-scale fading, path loss, delay, and other temporal and spectral dynamics of the link that act on the propagated electromagnetic signal in 2-D or 3-D dimensional. For that, the problem of solving the discontinuity, interference characteristics has been taken by many authors using more rigorous analytical techniques. Most of the techniques used to involve some large set of equations to be numerically solved[29]. The numerical solutions of these equations of different problems, which mentioned before, are invoked by analytical methods in its differential or integral forms which are widely used as solution for an electromagnetic radiation and scattering problems[30]. Among these integral methods, we can cite the surface integral equation method, the matrix boundary element method(BEM), the transmission line matrix method(TLM) and the reciprocity theorem which based on the method of moment. For the differential methods, it exists the Finite Difference(FD) method, the Finite Element Method(FEM). In this chapter, we will introduce the discontinuity problems in 3D space and the integral methods of resolution which based essentially on the reciprocity theorem. This one has proven to be an extremely powerful tool for solving a variety of electromagnetic problems.

2.2 Motivation and Problems Description

The introduction of new three-dimensional passive devices that yield higher package densities reducing the size, weight and cost necessitate progress in analysis and circuit design. Most of the commercially available software for the characterization of passive structures are based on models, or can only handle planar structures in the sense of a full-wave analysis. The use of the full-wave techniques[31] is to model accurately transmission line and discontinuities taking into account dispersion, mismatch, coupling effect, radiation, etc... For the first time, "the full-wave analysis of such real three-dimensional structures has to be done using the finite-difference approach[32] or the transmission line matrix method[33]". Up to now, other analytical methods are used such as the finite element method and the reciprocity theorem which based on the method of moment. The region to which this last one applies may consist of dissipative, dispersive, non-homogeneous, and an-isotropic media, and all these properties may extend to infinity. Based on this theorem a variational expression that provides an approximation for giving discontinuity characteristic by calculating scattered fields, current density distribution, and input impedance has been obtained. The meaning of the approximation for the previous parameters as arbitrary functions that verify the boundaries conditions of the studied structure.

2.3 Study of the discontinuity

Accurate, efficient and general computational techniques are developed to evaluate the scattering parameters of passive microstrip components composed of discontinu-

ities in microstrip structures. Geometrical discontinuities associated with these lines affect the circuit performance[34]. Various dimensions considered correspond to those of the planar models. Two-dimensional(2-D) analysis is used to analyze accurately the discontinuities. In recent years, a full-wave analysis that includes these physical effects has been developed for various microstrip planar structures discontinuities[35] in the space mentioned before and in the 3D space. Today, personal computers(PCs)are capable of performing calculations at speeds similar to the biggest computers of a few years ago. Hence, numerical techniques have become more practical for microwave CAD design. Still, even the supercomputers of today much faster and much more expensive than the PCs can be overwhelmed by brute force attempts to solve the partial differential or integral equations of general electromagnetics problems of modest complexity. Sorrentino states that when considering numerical methods, although computer efficiency increases with the amount of analytical preprocessing required, the versatility of the method is generally reduced. He acknowledges that most general structures can be attacked only by essentially numerical methods with no restriction on the type of geometry. Unfortunately, techniques in this category(FE, FD, general MOM, etc....)have the largest computer memory and calculations requirements. However, the modeling of discontinuity was viewed as being one of the key-bottleneck problems in the successful implementation of CAD. As an alternative, integral equation techniques for the analysis of integrated circuit discontinuities problems was done by individuals with interest in microstrip antenna technologies. Still the application of the techniques which cited above specifically to the problems of microstrip discontinuities can be date back only as far as 1985, when Jackson and Pozar and Katehi and Alexopoulos published their respective works on open-end and gap discontinuities[36] of different planar structures which excited with different type of excitation sources like planar source,modal source and coaxial cable source. This last one will be considered our basic source.
Transverse-electromagnetic (TEM) mode waves are conducted through a coaxial cable with very low loss compared to free-wave radiation and are resistant to outside signal interference. As there are many environments and applications were RF devices find themselves, coaxial cables need to be built to meet a range of challenges[37].

2.4 Integral Methods

2.4.1 Reciprocity Theorem

2.4.1.1 General Definition of Reciprocity Theorem

The principle of reciprocity finds a wide range of applications, from human relations to international trade, politics to science and engineering. Reciprocity denotes a mutual exchange between two interacting agents. Technically, it describes the reversibility or bilateral-ism of interaction upon interchange of the source and target. Although a loose statement of the principle is usually sufficient for many cases, a precise definition

is essential in science and engineering. The next subsection aims will discuss the reciprocity principle in electromagnetic engineering[38].

2.4.1.2 Reciprocity Theorem in Electromagnetic: Theory

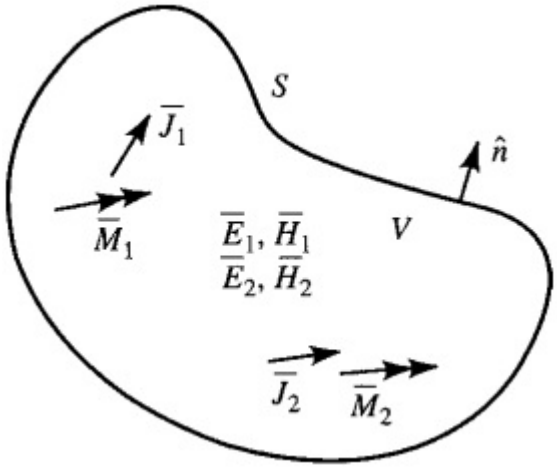

Figure 2.1: Geometry of Lorentz Reciprocity Theorem

Reciprocity is a general concept that occurs in many areas of physics and engineering, and the reader may already be familiar with the reciprocity theorem of circuit theory. Here, we will derive the Lorentz reciprocity theorem for electromagnetic fields in two different forms. This theorem will be used later in our manuscript to obtain general properties of network matrices representing the current and field values of microwave circuits. There are several other important uses of this powerful concept. Reciprocity theorems are among the most useful tools in field and circuit problems, ranking with the superposition theorem and the equivalence theorems. It is convenient to classify the reciprocity theorems into three types: pure circuit, pure field, and mixed circuit[39]. The pure circuit form developed by Rayleigh for networks of lumped elements was extended to antennas by Carson. It applies to a pair of antennas only if each antenna has suitable terminals where voltage and current can be defined in[40] by:

$$V_{12}I_{11} = V_{21}I_{22} \tag{2.1}$$

A theorem of the second type (pure field) involving electric and magnetic-fields intensities was derived by Lorentz in the form of the surface integral as shown in the following equation:

$$\int_{s_1} (E_1 \times H_2 - E_2 \times H_1) \cdot ds = \int_{s_2} (E_2 \times H_1 - E_1 \times H_2) \cdot ds \tag{2.2}$$

Where S_1 is the encloses surface of antenna 1 and S_2 is the encloses surface of antenna 2. Carson also presented a pure field theorem in the form of a volume integral involving electric-current density and electric-field intensity.

$$\int_{V_1} J_1 \cdot E_2 d\tau = \int_{V_2} J_2 \cdot E_1 d\tau \tag{2.3}$$

Where volume V_1 includes antenna 1 and V_2 includes antenna 2. Rumsey has given the name "reaction" to the quantity represented by the integrals which appear in the Lorentz reciprocity theorems and Carson has proposed the symbol$\langle 1, 2 \rangle$ for the integrals on the left side in (2.2) and (2.3). However, if the conditions of reciprocity are satisfied, this reaction theorem can be combined with any one of the "pure" reciprocity theorems given above to obtain a reciprocity theorem of the "mixed type". Circuit quantities (voltage and current) appear on one side of the equation, while field quantities appear on the other side. Thus, the general formulation of reciprocity theorem is based on Maxwell's equations. Considering, two types of sources J^a, M^a and J^b, M^b which has the same frequency and existing in the same linear plane. The electromagnetic fields which produced by source "1" are E^a, H^a and with source "2" are E^b, H^b as mentioned in this equation.

$$\begin{cases} \{J_a, M_a\} \rightarrow \{E^a, H^a\} \\ \{J_b, M_b\} \rightarrow \left\{E^b, H^b\right\} \end{cases} \tag{2.4}$$

The relations between electromagnetic fields are given by the below equation:

$$\nabla \times H^a = \widehat{y}E^a + J^a \quad \nabla \times H^b = \hat{y}E^b + J^b \quad \nabla \times E^a = \hat{z}H^a + M^a \quad \nabla \times E^b = \widehat{z}H^b + M^b \tag{2.5}$$

We multiply the first scalar by E^b and the last one by H^a and add the resulting equation, we obtained:
$-\nabla \cdot \left(E^b \times H^a\right) = \hat{y}E^a \cdot E^b + \hat{z}H^a \cdot H^b + E^b \cdot J^a + H^a \cdot M^b$
where the left hand term has been simplified by the identity. Hence, the interchange of two sources "a" which corresponds to the source "1" and "b" which corresponds to the source "2" and a subtraction of the former equation from the latter given:

$$\begin{aligned} &-\nabla \cdot \left(E^a \times H^b - E^b \times H^a\right) \\ &= E^a \cdot J^b + H^b \cdot M^a - E^b \cdot J^a - H^a \cdot M^b \end{aligned} \tag{2.6}$$

This equation is named the Lorentz Reciprocity Theorem, its integral form is given by the below equation:

$$\begin{aligned} &\oiint \left(E^a \times H^b - E^b \times H^a\right) dS \\ &= \iiint \left(E^a \times J^b - H^a \times M^b - E^b \times J^a + H^b \times M^a\right) d\tau \end{aligned} \tag{2.7}$$

Let us consider that all sources and components are of finite extent, so the left-hand term of equation(**??**) is equal to zero and its new expression is given by:

$$\begin{aligned} &\iiint \left(E^a \times J^b - H^a \times M^b\right) d\tau = \\ &\iiint \left(E^b \times J^a - H^b \times M^a\right) d\tau \end{aligned} \tag{2.8}$$

This is the general form of the Reciprocity Theorem in the electromagnetic field and the most useful. Thereafter, we will apply that one to our analysis structure which will be studied in the next chapter.

2.4.1.3 Historic of Reciprocity Theorem

The reciprocity theorem was presented by Lord Rayleigh in 1894[41] who was discovered the original proof of the reciprocity theorem, which is stated by him in the language of electric circuit theory as follows: "Let there be two circuits of insulated wire A and B, and in their neighborhood any combination of wire circuits or solid conductors in communication with condensers. A periodic electromotive force in the circuit A will give rise to the same current in B as would be excited in A if the electromotive force operated in B". Before proceeding with the generalization. Rayleigh's theorem, in the following modified form, will be stated and proved. Hence, he has

proven its utility in communication engineering and it has been applied only to quasi-stationary transducers that have obeyed simple laws of electrical circuit theory[42]. For electromagnetism relations[43], Hendrik Antoon Lorentz (Nobel Prize winner in 1905), who was in 1896 gave the mathematical formulation of the reciprocity principle for electromagnetic fields. He has indeed proved that it is a powerful tool for solving many of the theoretical and practical electromagnetic problems[44]. His theorem applies the propagation light vibration to time harmonic field. Following Guglielmo Marconi's success in 1895 in demonstrating the possibility of sending and receiving signals using electromagnetic waves, radio communication research boomed[45]. A reciprocity theorem for electromagnetic fields was very much needed, particularly to understand the behavior of transmitting and receiving antennas. In July 1924[46], it was the journal subject named "The "Bell System Technical Journal" whose author is declared and proved the general object of reciprocity theorem. However, to the limitation that the permeability must be the same in every point of medium. Later, Pleijel declared the theorem for unlimited values of discussing the reciprocity theorem in June 1929 from "The Proc. I.R.E.". Over the years, these two theorems of Rayleigh and Lorentz have been elucidated and extended by several authors[47]. A version of these theorems specialized to the case of harmonic time dependence is now included in many textbooks in electromagnetic theory. Moreover, the interaction quantity that occurs in Lorentz's reciprocity theorem was later denoted by Rumsey in 1954 as the "reaction" between source and fields in the two states. In their analyses, H.A.Lorentz's and Rumsey incorporated general reciprocal an-isotropic and lossy media. Consequently, the first detailed discussion of a reciprocity theorem for electromagnetic fields with arbitrary time dependence was given in a paper which written by Welch in 1960, some 64 years after the paper of Lorentz[48], Welch's[49, 50]paper was quickly followed by others presenting different formulations. Furthermore, Ballantine, whose name lives on in the Stuart Ballantine Medal, published a most important application of the field reciprocity theorem, referring to important work carried out by Raymond M. Wilmotte of the National Physics Laboratory in the U.K. A convolution type of the reciprocity theorem applying to general causal dispersive media was presented by Ru-Shao Cheo(1965)[51]. His proof based on space-time arguments only. Geurst(1963) had earlier derived a similar reciprocity relation, using, however, the Time Fourier Transform in the intermediate step. Bojarski(1983) clearly distinguished between convolution- and correlation-type and presented the corresponding time domain reciprocity theorems for homogeneous, isotropic, and lossless media, where the electromagnetic field is easily expressible in terms of its scalar and vector potentials (in the Lorentz gauge) and where the electromagnetic Green's dyadic is shift-invariant in space-time. The application of reciprocity theorems to radiating apertures was studied by Van Bladel(1966). Hoop(1959) investigated their application to the direct scattering of electromagnetic waves and to multi-port antenna(1975). As we will show below, this application leads to a hybrid reciprocity theorem that is of importance when considering antenna factors, radiated emission and immunity mea-

surements, shielding effectiveness and uncertainties in EMC measurements.
Here the meaning of "hybrid" is that, mathematically, the theorem is expressed in terms of voltage and current, on the one hand, and in electric and magnetic field components, on the other hand.

2.4.1.4 Some Applications of Reciprocity Theorem

The earliest days of radio communication, the reciprocity theorems of Rayleigh and Lorentz have been applied to the antenna problems especially[52, 53]. After that, it has been used for several applications of which we can cite: a printed slot fed by a microstrip line which it concentrated on the study of the interference between pcb electronics components[54–56]. Another application, the reciprocity theorem has been applied to simplify the calculations[42] of the interactions of the electromagnetic dispersion's from an existing target on a rough surface[57–59]. Hence, the reciprocity technique is used to calculate the radiations of some form of microstrip antenna located on a dielectric and covered by cylindrical surfaces on it. We can quote that the technique of reciprocity was used to calculate the electromagnetic coupling in emission and in reception of a reflector antenna[60].For that, the aim application of the reciprocity theorem is to calculate the far electric field existing in the surface which cover the plane space of structure.
The major advantage of this method is that it does not require the tedious evaluation of complicated media.

2.4.2 Method of Moment

Harrington was introduced the general moment method to the electromagnetics area when it had already been applied to specific problems by Mei and Van Blade1, Andreasen, Richmond, Waterman, and others. Since then, the moment method has been widely adopted for solving electromagnetic problems like radiation and dispersion via the integral-equation approach[61]. The method of moments (MoM) has been recognized as one of the most powerful candidates for accurate and efficient modeling of planar circuits. It is a technique used to solve the electromagnetic problems at the borders or the integral equations in volume in the frequency domain[62]. It is a matrix method.

2.4.2.1 Historic

In 1967[63], Harrington introduced the method of moments for solving problems related to antennas. This numerical method consists of transforming a problem (differential or integral equation) into a system of linear equations. In electromagnetic, the method of moments consists of solving the integral formulation of the Maxwell equations, in the temporal or spectral domain.
Principle:

- The current density on the antenna is the variable considered.
- From the current density, all the parameters of the antenna can be deduced.
- The current density is discretized into a set of elements called basic functions where the amplitudes are unknowns to be determined.
- Boundaries conditions for electric and magnetic fields are reinforced on the surface of the element using the test functions.

2.4.2.2 Definition

The method of moments is a general concept that we can apply to numerical or analytic concepts[64]. This method makes it possible to determine the current distribution as well as the field in planar or closed environments[65–68]. It solves an equation of form

$$\Gamma f = g \tag{2.9}$$

Γ is the Hilbert operator on a free space, f is the unknown problem function and g is a given function that represents the excitation. Consequently, the method of moment makes it possible to obtain an approximation by an inversion of Γ^{-1}, hence an approximation of f.

2.4.3 Equivalent Circuit Generalized Method

The Generalized Equivalent Circuit Method (GEC) is an integral method[69, 70] that models a given structure with an equivalent electrical scheme in terms of the impedance and admittance operators. It solves Maxwell's equations on the surface of the discontinuity.

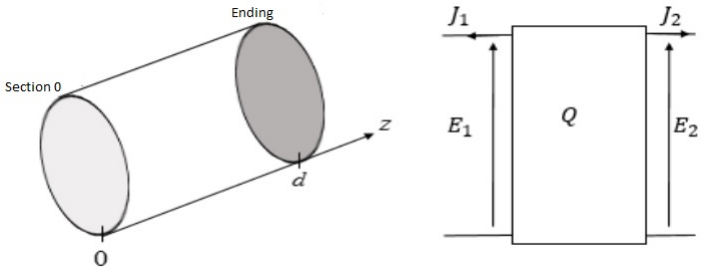

Figure 2.2: Modeling with Equivalent Generalized Circuit

2.5 Objectives and Contributions

An integral equation for the discontinuity is written by enforcing the boundary condition that the total 2 electric field due to all the currents on the line must be zero

on the line. A significant amount of work has been invested and oriented essentially the analysis and modeling of a class of planar discontinuities that are bounded in a metallic enclosure.

2.6 Conclusion

In this chapter, we announced the discontinuity problems existing in planar structures especially in a 3D plane and their difficulties of resolution. we started with a brief description of our aim work. In a second way, we gave the analytical tools based essentially on the reciprocity theorem which also based on the method of moment for analyzing and modeling the 3D discontinuity combined with MGEC. Thirdly, we defined the reciprocity theorem in the general case and its different applications. But before that, we described the excitation source which will be used in the next chapters. In what follows, we will detail the formulation of reciprocity theorem and we will validate that with a simple structure.

Chapter 3

Reciprocity Theorem Application

Contents

3.1 Introduction

The practical advantages of microstrip structures have been discussed in many papers. On the other hand, it is perhaps worthwhile to point out that such structures are very well suited for mathematical modeling. This seldom mentioned "theoretical" advantage is mostly due to the relatively simple geometry of microstrip structures and has certainly contributed to their popularity. Indeed, every analytical techniques commonly used in electromagnetic has been applied to microstrip, giving rise to a surprisingly great number of different and unrelated models. In this chapter, the basic mainstream of the validation process of analytical technique which is based on the reciprocity theorem can be detailed then explored. To show how it could be important using such a reciprocity theorem(RT) within the electromagnetic field. After all whole things of exploration, the formulation of the main problem would be explicitly defined to turn this work into operative balancing behavior of sight satisfaction with the required ideas of using digital concept.

3.2 Structure Description

We will study the structure given by the figure below:
It described by a microstrip resonator injected in an open-end metallic waveguide.

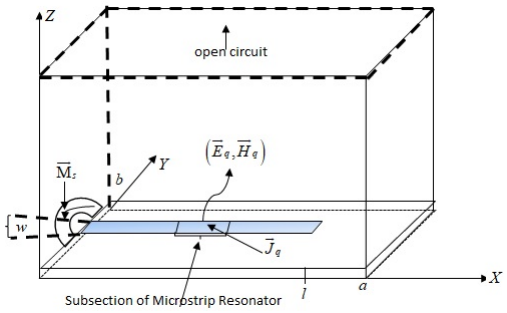

Figure 3.1: *Descriptive Schema of Structure Excited with Coaxial Source sizing:* $a(waveguidelength)$=47.55mm,$b(waveguidewidth)$=22.15mm,h=1.5mm,$l(length_{strip})=\lambda_g/4$, $w(width_{strip})$=2.8mm,ϵ_r=4.32,$freq$=6.9GHz,$r(outerradiuscoaxial)$=2.7mm.

The microstrip resonator was excited by a coaxial cable which introduces a magnetic current source noted M_s existing in the aperture of the cable. The source induces the current distribution J_s on the conducting microstrip resonator and produces the total electric field E^{tot} and the total magnetic field H^{tot} inside an open-end waveguide. Hence, an auxiliary source that exists in a subsection of microstrip resonator denoted J_q named test current that induces the auxiliary electric field E_q and auxiliary magnetic field H_q as indicated in Figure(3.1).

3.3 Development of Reciprocity Theorem Attached to GEC Method

In this section, we will develop the numerical techniques used for calculating structure parameters of Figure(3.1).

3.3.1 Definition of Reciprocity Theorem

Let suppose two pairs of sources which is given by:

$$\begin{cases} \{J_a, M_a\} \rightarrow \{E^a, H^a\} \\ \{J_b, M_b\} \rightarrow \left\{E^b, H^b\right\} \end{cases} \tag{3.1}$$

The general form of reciprocity theorem (reciprocity theorem is the reaction between two different sources) is given by the below equation:

$$\left(\iiint_V E^a \cdot J_b - H^a \cdot M_b - E^b \cdot J_a + H^b \cdot M_b \right) dV = 0 \tag{3.2}$$

Equation(3.2) is named Reciprocity Theorem of Lorentz.

3.3.2 Generalized Equivalent Circuit Method

All numerical methods are based on Maxwell equations which defines the physical laws governing the electrical and magnetic field in time and space variation[71]. They(mean numerical methods)differ in solving these equations. To lighten the resolution of these equations, the Generalised Equivalent Circuit Method noted GECM or MGEC which was produced by H. Baudrand[72]. It used to modulate the integral equations by an equivalent electric circuit. This method represents an extension of integral equations based on a transposition field problem into electrical circuit problems. The idea arises from an analogy between equations describing boundaries conditions of an electromagnetic state (current and field) on a discontinuity interface, and that highlighting voltage and intensity in a circuit[73, 74]. This modeling allows extending Kirchoff laws used with the concept(V, I) in Maxwell's formalism(E, H)[75].

3.3.3 Theory

The resolution of our problem is given by this organigram which describes different steps of analysis.

Now, we consider these excitation sources of subsection one which describe our case and which replaces by this couple of sources (M_s, J_s) and J_q. The electromagnetic

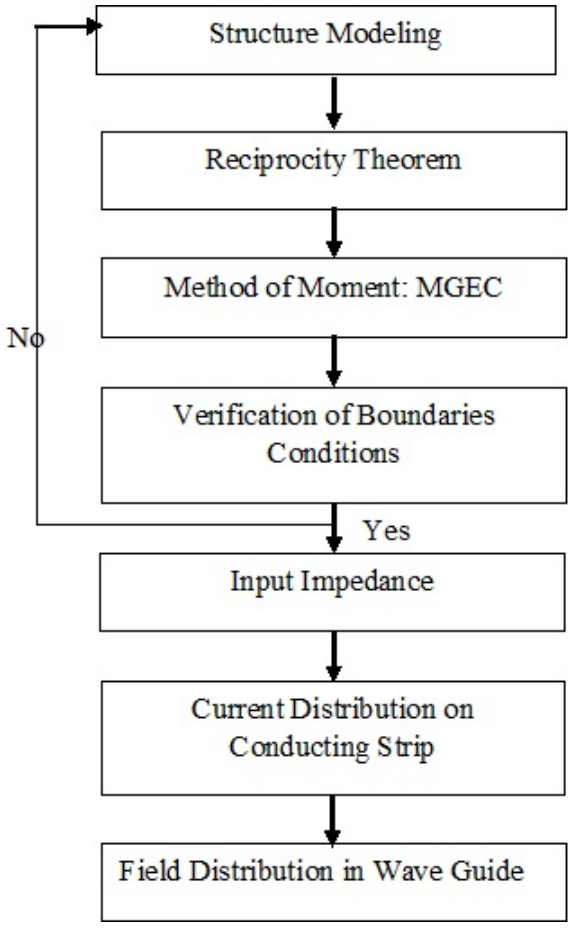

Figure 3.2: *Descriptive Algorithm of Reciprocity Theorem.*

fields produced by the first source are noted E^{tot} and H^{tot}, and by the second source are noted E_q and H_q. Applying the reciprocity theorem, the relation between the electromagnetic fields is given by:

$$\iiint_V \left(\vec{E}^{tot} \cdot \vec{J}_q - \vec{E}_q \cdot \vec{J}_s - \vec{H}_q \cdot \vec{M}_s\right) \cdot dV = 0 \tag{3.3}$$

Where V represent the inside waveguide volume. So, the previous equation can be written as:

$$\iiint_V \left(\vec{E}^{tot} \cdot \vec{J}_q\right) \cdot dV = \iiint_V \left(\vec{E}_q \cdot \vec{J}_s - \vec{H}_q \cdot \vec{M}_s\right) \cdot dV \tag{3.4}$$

By simplifying the 1st term of previous integral $\left(\vec{E}^{tot} \cdot \vec{J}_q\right) = 0$, of equation(3.4) because the test current J_q exists only in the subsection of microstrip resonator and

in the other hand E^{tot} coverage the hole waveguide volume. So, the tangential component is null. A new equation is given by equation(3.5):

$$\iiint_V \left(\overrightarrow{E}_q \cdot \overrightarrow{J}_s\right) \cdot dV = \iiint_V \left(\overrightarrow{H}_q \cdot \overrightarrow{M}_s\right) \cdot dV \tag{3.5}$$

Using the reciprocity theorem, we can reduce the volume integral to surface integral, such that:

$$\iint \left(\overrightarrow{E}_q \cdot \overrightarrow{J}_s\right) dS = \iint \left(\overrightarrow{M}_s \cdot \overrightarrow{H}_q\right) dS \tag{3.6}$$

Hence, the auxiliary electric field E_q will be calculated in the plane which z=0 and the auxiliary magnetic field H_q in the plane which x=0 as shown in the below equation:

$$\iint_{S_{resonator}} \overrightarrow{E}_q\,(z=0) \cdot \overrightarrow{J}_s \cdot dS_{resonator} = \iint_{S_{feed(coaxial)}} \overrightarrow{H}_q\,(x=0) \cdot \overrightarrow{M}_s \cdot dS_{coaxial} \tag{3.7}$$

where $S_{resonator} = (xoy)\,plane$ and $S_{feed(coaxial)} = (yoz)\,plane$.

3.3.3.1 Integrals Elements

The test current J_q is defined by:

$$J_q = I_q \cdot g_q \tag{3.8}$$

where I_q is the magnitude of J_q and g_q represent the basis function of microstrip resonator subsection and it defined by echelon function(3.9) as shown in Figure(3.3):

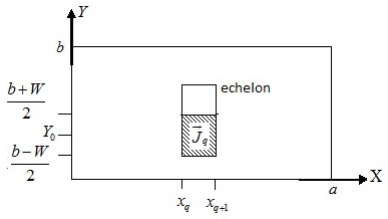

Figure 3.3: *Test Function Definition of Subsection.*

$$g_q(x) = \begin{cases} 1 & if \quad x_q \le x \le x_{q+1} \quad \& \quad \dfrac{b-w}{2} \le y \le \dfrac{b+w}{2} \\ 0 & others \end{cases} \tag{3.9}$$

The current distribution density of equation(3.10) which exists in microstrip resonator is given by:

$$\overrightarrow{J}_s = \sum_p I_p \cdot g_p(x,y)\,\overrightarrow{x} \tag{3.10}$$

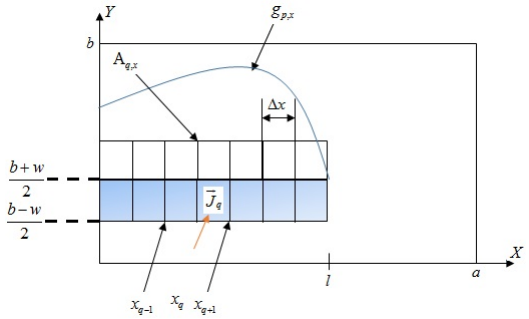

Figure 3.4: *Test Function Definition.*

where I_p represent the vector of unknown coefficients, g_p is the test function which has been chosen to verify boundaries conditions of metallic waveguide. It defined by the Figure(3.4) and equation(3.11):

$$g_p(x,y) \begin{cases} \cos\left(\dfrac{(2p-1)\,\pi}{2l}x\right) & if \quad 0 \le x \le l \quad \& \quad \dfrac{b-w}{2} \le y \le \dfrac{b+w}{2} \\ 0 & others \end{cases} \tag{3.11}$$

By applying the Generalized Equivalent Circuit Method (MGEC) which shown in Figure(3.5), the auxiliary electric field could be expressed such that:

$$E_q = \hat{Y}_{eq}^{-1} \cdot J_q = \hat{Y}_{eq}^{-1} \cdot I_q \cdot g_q \tag{3.12}$$

And the auxiliary magnetic field is given by the below equation which is based on Maxwell-Fraraday laws:

$$\overrightarrow{H}_q = \frac{j}{w\mu_0}\overrightarrow{rot}E_q \tag{3.13}$$

3.3.4 System Resolution

Basing of integral form which defined by equation(3.7), we can transform the integral form to product scalar in the below equation:

$$\langle E_q(z=0), J_s \rangle = \langle H_q(x=0), M_s \rangle \tag{3.14}$$

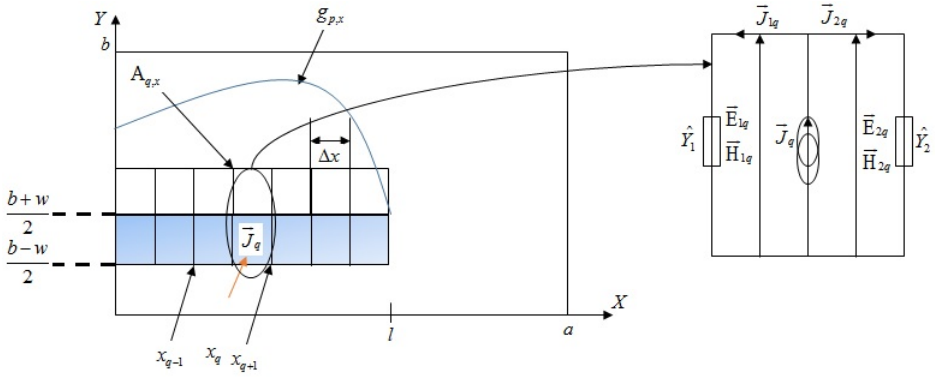

Figure 3.5: *Equivalent Circuit of Subsection.*

We can also write:

$$\left\langle E_q\left(z=0\right), \sum_p I_p \cdot g_p \right\rangle = \left\langle H_q\left(x=0\right), M_s \right\rangle \tag{3.15}$$

Multiplying the equation(3.15) by the coefficientI_q, we obtained the below equation:

$$\sum_{p,q} I_p I_q \left\langle E_q\left(z=0\right), g_p \right\rangle = \sum_{p,q} I_q \left\langle H_q\left(x=0\right), M_s \right\rangle \tag{3.16}$$

Which, it can be transformed to:

$$\left[\left\langle E_q^{'}\left(z=0\right), g_p \right\rangle\right] \cdot \left[I_p\right] = \left[\left\langle H_q^{'}\left(x=0\right), M_s \right\rangle\right] \tag{3.17}$$

$E_q^{'} = I_q E_q$, $H_q^{'} = I_q H_q$ and the magnetic current source is defined by:

$$\overrightarrow{M}_s = -\frac{V_0}{\rho \ln\left(\frac{r_b}{r_a}\right)} \overrightarrow{\phi} \tag{3.18}$$

with $\overrightarrow{\phi} = \rho d\rho d\varphi$(in cylindrical coordinates).
The main principles of solving linear systems like $AX = B$ which should ask for constraint conditions to satisfy some proposals and then to invoke the mainstream mechanism of boundary conditions limit theory to can vary some values from initial values to desirable values to non-desirable values to infinite or semi finite and so on. This could help people understand the meaningfulness of solving signal complexity and building a great bridge deal of entire excitement could figure out any associate assignment of trustfulness and hopefulness. Thus, this proposal table could then return the operative occurrence of some solutions that would be used along over away.

$A = \left[E_q^{'}, g_p\right]_{\text{Matrix for impedance variations}}$	$B = \left[H_q^{'}, M_s\right]_{\text{Excitation vector}}$
$X = [I_p]_{\text{Vector for ponderation show}}$	$[I_p] = \sum_{p,q} \left[H_q^{'}, M_s\right] \cdot \left[E_q^{'}, g_p\right]^{-1}_{\text{Solution}}$

3.3.5 Element Computation of Linear System

3.3.5.1 Computation of Matrix Element A

The matrix values could be determined using this equation such that: Although much

$A = \sum_{p,q} \left[\left\langle E_q^{'} \middle| g_p \right\rangle\right] = \sum_{p,q} \left[\left\langle \hat{Y}^{-1} g_q \middle| g_p \right\rangle\right]$	$\hat{Y}^{-1} = \sum_{m,n} \left\lvert f_{mn}^{TE,TM} \right\rangle y_{mn}^{-1(TE,TM)} \left\langle f_{mn}^{TE,TM} \right\rvert$

more detailed designs of solving the problem of impedance's values could be found in appendix B, but its final value for the TE mode and TM mode could be given by this equation as flowing:

$$A = \sum_{p,q} \sum_{m,n} \langle g_p, f_{mn} \rangle^{TE,TM} y_{mn}^{-1} \langle f_{mn}, g_q \rangle^{TE,TM} \tag{3.19}$$

3.3.5.2 Computation of Excitation Vector B

The excitation vector B could be given by this equation such that:

$$B = \left[M_s, H_q^{'}\left(x = 0\right)\right] \tag{3.20}$$

The computation details of are given in appendix C and which obtained this expression:

$$\begin{aligned} B &= \sum_q \left\langle M_s, H_q^{'} \right\rangle_i = \sum_q \left\langle \left(M_{sy} + M_{sz}\right), \left(H_{qy}^{'} + H_{qz}^{'}\right) \right\rangle_i \\ &= \sum_q \left\langle M_{sy}, H_{qy}^{'} \right\rangle_i + \sum_q \left\langle M_{sz}, H_{qz}^{'} \right\rangle_i \end{aligned} \tag{3.21}$$

Where i= region (1,2) of the source. The source excitation vector will be calculated for all propagation modes. Thereof, from the element matrix and excitation vector values, we will give the current distribution density as well as electric field distribution of microstrip resonator.

3.4 Current Distribution Density J_s and Electric Field distribution E_x

The current distribution density of the microstrip resonator is given by:

$$J_x(x,y) = \left(\sum_{p,q} \left(\sum_{m,n} I_p \langle g_p(x,y), f_{mn} \rangle f_{mn} \right)^{TE} + \sum_{p,q} \left(\sum_{m,n} I_p \langle g_p(x,y), f_{mn} \rangle f_{mn} \right)^{TM} \right) \overrightarrow{x} \tag{3.22}$$

The electric field distribution of an open waveguive in (xoy) plane is following by:

$$\overrightarrow{E}_x = \widehat{Y}^{TE,TM} J_x \overrightarrow{x} \tag{3.23}$$

3.5 Results and discussions

In this section, we will give reciprocity theorem results which applied on microstrip resonator.

3.5.1 Study of convergence

We start by studying the convergence of numerical results of coaxial excitement in order to calculate the current density and field distributions appropriately at the frequency equal to $6.9GHz$. For reaching the convergence, we need to increase the modal functions number by fixing the test functions number. The convergence is reached for modal functions $M = N = 300$ and test functions $P = Q = 10$. Hence, we will consider these values to model the structure excited by the coaxial cable given in this work.

3.5.2 Current Distribution

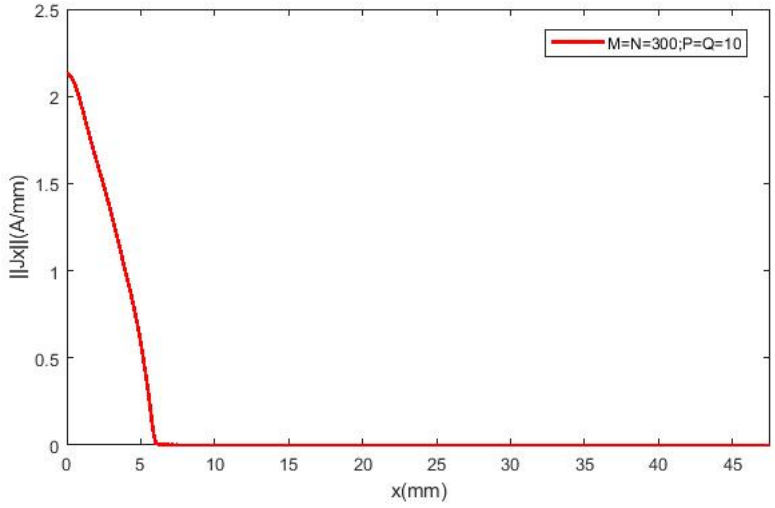

Figure 3.6: *Current Density Distribution.*

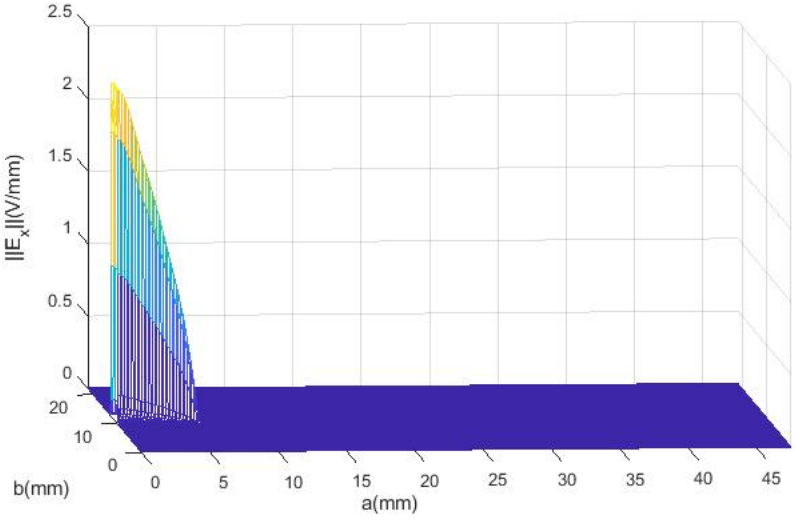

Figure 3.7: *Current Density in 3D Space.*

Let's take a look at this driven distribution of current density, it is assumed to notice that the above graphic could ask of its variation along the microstrip line resonator. The value of current distribution density is given by this Figure(3.6) for microstrip resonator length equal to $\frac{\lambda_g}{4}$ at frequency equal to $6.9GHz$. We noticed that the current value verifies the boundary condition of metallic waveguide. It's maximum on the metallic microstrip resonator and null.

3.5.3 Electrical Field Distribution

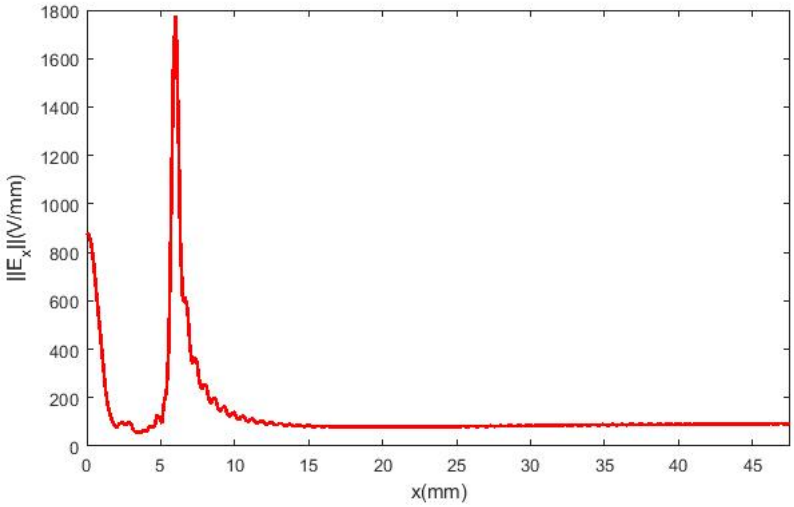

Figure 3.8: *Electric Field Distribution in* (xoy) *Plane in Convergence.*

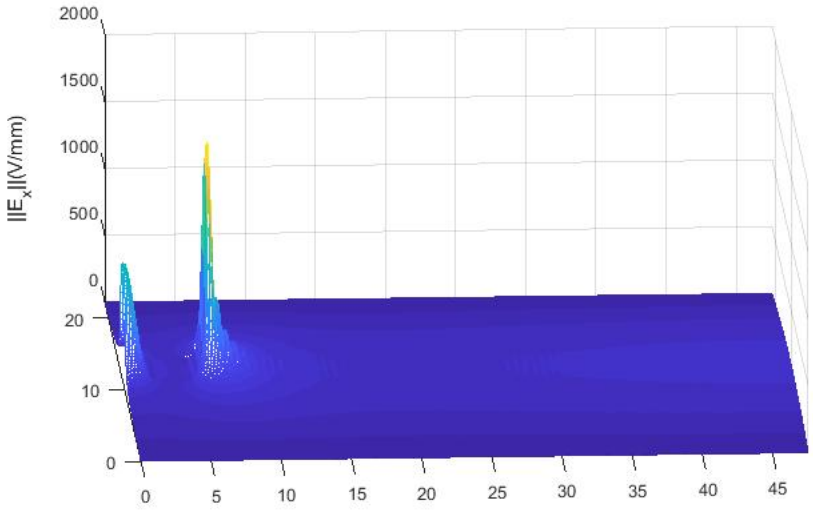

Figure 3.9: *Density of 3D-Electrical Field Distribution in* (xoy) *plane of Coaxial Source in Convergence.*

Figure(3.8) and Figure(3.9) show the behavior of electric field for coaxial source. We noticed that the electric field is maximum near the coaxial source and on the dielectric, despite it is near to zero on metallic microstrip resonator. This small value of electric field is explained by the existing of discontinuity which is not well modeled. Hence, its behavior verifies the boundary condition of an open-end metallic waveguide. The below figure shows the behavior of electric field distribution in (yoz) waveguide plane with variation of its height in function of the wavelength λ_g.

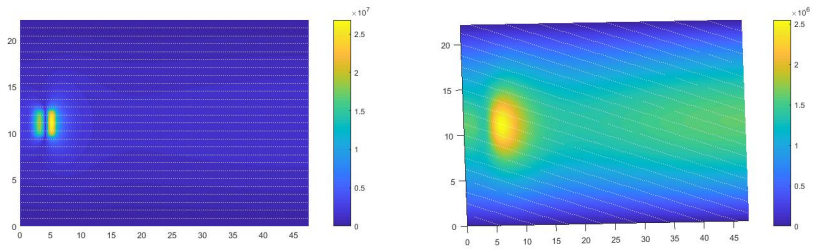

(a) $z = 0$ (b) $z = {}^{\lambda_g}/_{8}$

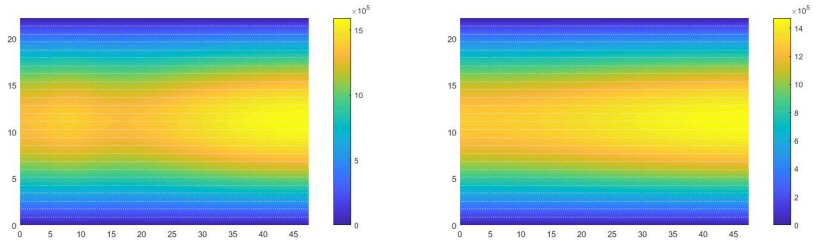

(c) $z = {}^{\lambda_g}/_{3}$ (d) $z = \lambda_g$

Figure 3.10: *Electric Field Distribution by Varying the Height of the Waveguide*

3.5.4 Value of Z_{in}

3.5.5 Theory

The input impedance of microstrip resonator excited by coaxial cable is given by the flowing expression:

$$Z_{in} = \frac{\langle M_s, H \rangle}{\langle H, H \rangle} \tag{3.24}$$

where $E = \left(\hat{Y}_1 + \hat{Y}_2\right)^{-1} \cdot J_s$ and $\overrightarrow{H} = -\frac{1}{j\omega\mu_0}\overrightarrow{rot}\overrightarrow{E}$.

3.5.6 Results and Discussion

Figure(3.11) gives the value of input impedance. We noticed that the resonance frequency value of coaxial source case is equal to 7.3GHz. In figure(b) and figure(c), we compare the imaginary and real part of the input impedance to those found by HFSS simulation such as the resonance value is equal to 7.2GHz. Consequently, the two graphs have approximately an agreement. This agreement is provided by the value of relative error between the theoretical and simulation which is given by equation(3.25) and it's equal to 0.6%.

$$\delta_{\alpha_T} = \frac{|absulate\_value|}{theoritical\_value} \tag{3.25}$$

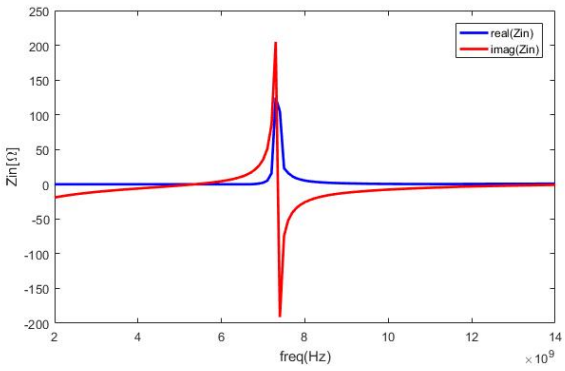

(a) *Value of Z_{in} of Coaxial Source*

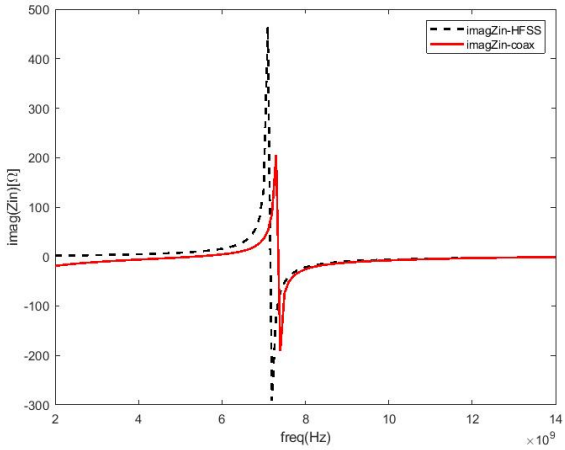

(b) *Imaginary Z_{in} of Coaxial Source(Reciprocity-HFSS)*

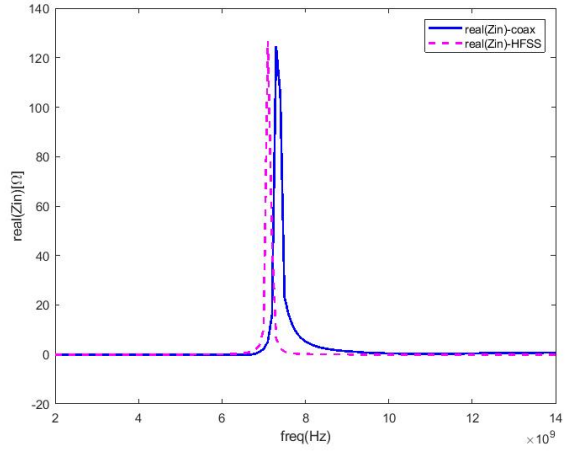

(c) *Real Z_{in} of Coaxial Source(Reciprocity-HFSS)*

Figure 3.11: *The Value (a) of Input Impedance and Comparison Between Imaginary Part Z_{in} of Microstrip Resonator Excited by: (b) Coaxial Cable with HFSS, (c) Real Z_{in} with HFSS and (d) Input Impedance Seen by Fundamental Mode*

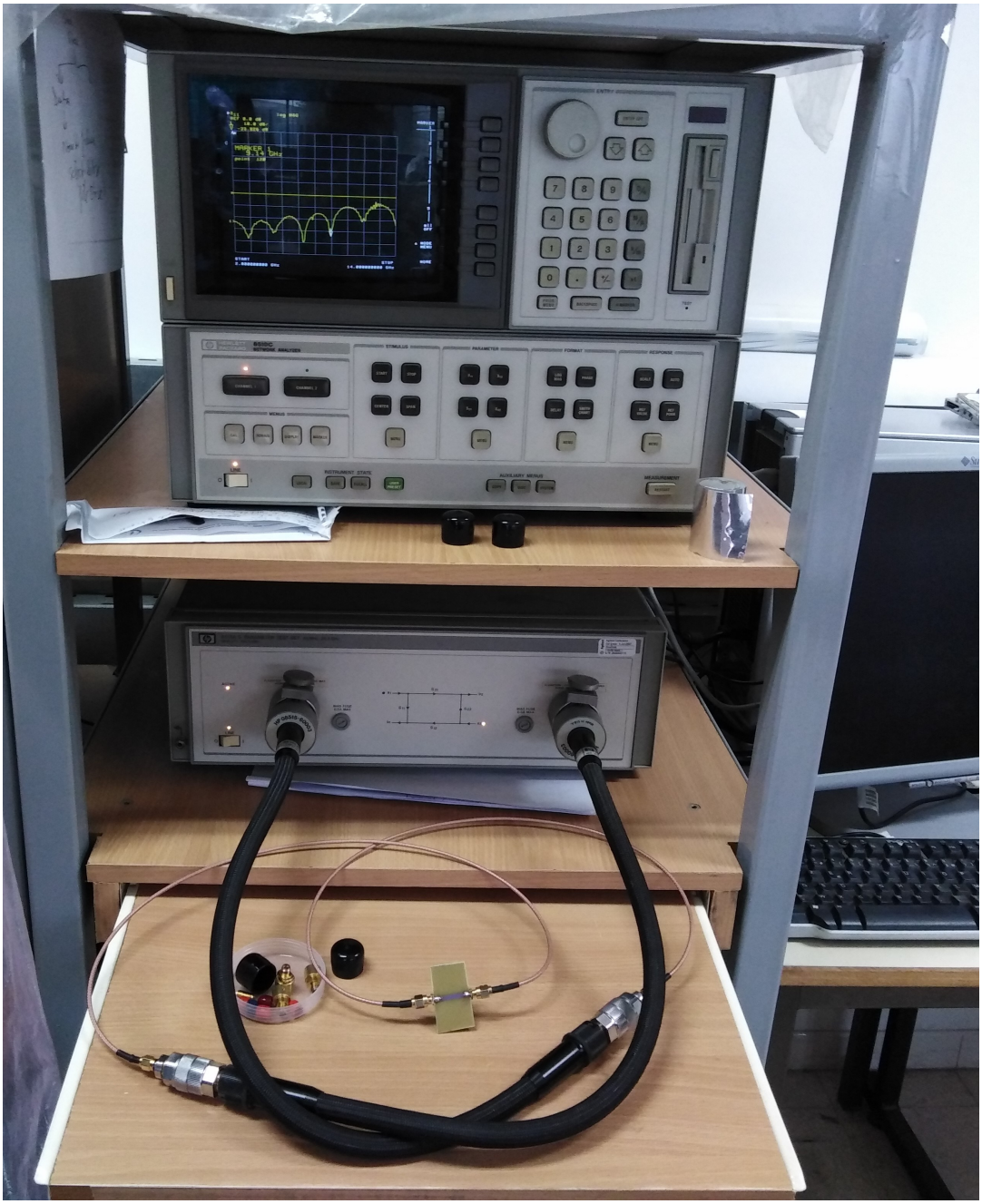

Figure 3.12: *Measurement of Microstrip Line Resonator.*

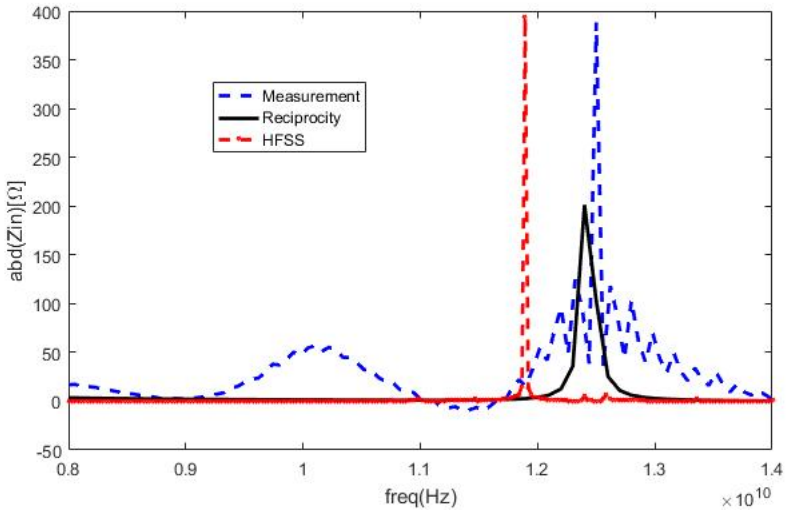

Figure 3.13: *Comparison of Input Impedance Value with Measurement.*

Due to theoretical and simulation results of input impedance that compared to measurement which is realized. Figure(3.12) showed the microstrip resonator connected to analyzer network. The calibration of this network is focused. In addition, in Figure(3.13), we have given the input impedance value in module obtained by measurement and HFSS simulation for the same structure conditions of Figure(3.12). We noticed that the two graphs are in concordance and has the same magnitude. On the other hand, the slight frequency difference value is explained by the measurement conditions and the materials used. This figure shown an agreement for a resonant frequency equal to 12GHz between our results which obtained by our method and those obtained by measurements. Those are observed with new dimensions in length and width of microstrip resonator quiet higher than those of the previous simulations and which are compatible with that of measurement environment. the new dimensioning of the waveguide ($90.5mm \times 22.15mm$) for HFSS simulation case make possible to overcome the electromagnetic coupling effect between the structure and the waveguide. Numerically, the test function number used for our method(which is proportional to computational time) is evaluated to 328 test functions while HFSS has not yet reached the desired convergence solution for 388 test functions.

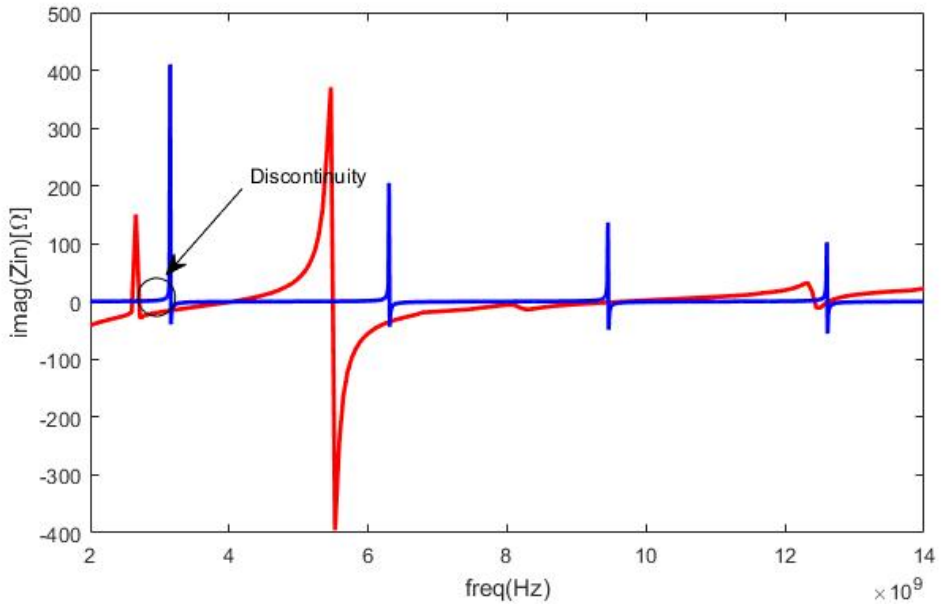

Figure 3.14: Imaginary Z_{in} Seen by Fundamental Mode of Propagation

Figure(3.14) presents the input impedance of source compared to that seen by the fundamental mode. However the impedance of the fundamental is defined in β variation as $Z_l = jZ_c \coth(\beta l)$. However, these graphs show an offset of resonance in which the input impedance is in quadrature phase advance compared to that seen by fundamental mode. However, the first resonance is equal to 2GHz. So, this allows the existence of discontinuity between coaxial source and the structure.

3.6 Conclusion

The integral method which based on the reciprocity theorem combined with GECM is a very convenient tool for studying microstrip structure. We have applied this method on a microstrip resonator which excited by a coaxial cable. We have shown the value in current, electric field distribution as well as the input impedance which has an agreement with those found by HFSS simulation and measurement. However, the comparison of the imaginary part of input impedance with that found by fundamental mode shows the existence of discontinuity between source and structure. This discontinuity will be studied in the next chapter. Finally, this technique(reciprocity combined with MGEC) can be applied to obtain the equivalent electric circuit of any microstrip structure.

Chapter 4

Discontinuity Analysis by Reciprocity Theorem and MGEC

Contents

4.1 Introduction

THE problem of electromagnetic(EM) propagation in stratified isotropic and anisotropic media has been studied extensively. A versatile work was evaluated the static analysis gaps in microstrip, gaps, and steps and other microstrip discontinuities. The fast computation time is taken by the RF structure in the electromagnetic field and the complexity of the integral equation solution needs to model the real source with its mathematical one to minimize the computation time. In the first section of this chapter, we will study the discontinuity existing between the excitation source and radiation element which studied in the previous chapter. In the second section, we will apply the reciprocity technique on the structure studied in the previous chapter but at this time we will replace the coaxial source by a planar one.

4.2 Study of Discontinuity

In this section, we will study the existence discontinuity between source and microstrip resonator. We will give the electric equivalent discontinuity circuit and give its parameter values.

4.2.1 Theory

4.2.1.1 Homographical Relation

To resolve discontinuity[76–79] problems existing between source and the planar structure, we try to give it a coupling circuit. The planar shorted-circuit structure, allows us to validate the variation of input impedance given by equation(3.24) in the previous chapter. When the shorted-circuit was placed away from, the reflected higher propagation mode was disappeared. In that case, we compare the numerical values given by equation(3.24) of the previous chapter with the following theoretical expression of reduced input impedance seen by the line and given by the following expression:

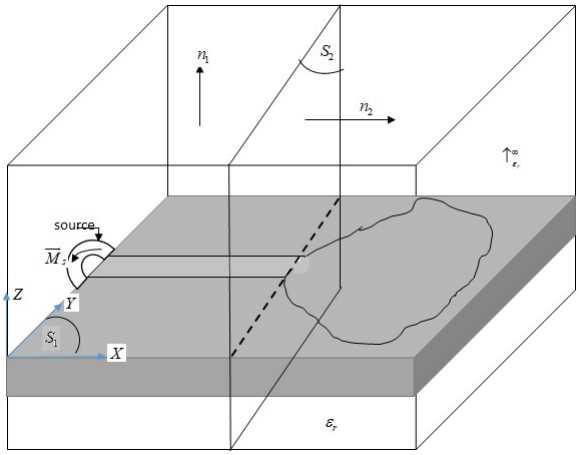

Figure 4.1: *Planar Circuit Excited by Source of Current*

The planar shorted-circuit structure, allows us to validate the variation of input impedance given by equation(3.24) which cited in previous chapter. When the shorted-circuit was placed away from, the reflected higher propagation mode was disappeared. In that case, we compare the numerical values with the following theoretical expression of reduced input impedance seen by the line and given by the following expression:

$$z_l = j \tan(\beta_g l) \tag{4.1}$$

Where l represents the length of the microstrip resonator and β_g is the propagation constant. This one is defined by: $\beta_g = \frac{2\pi}{\lambda_g}$, where $\lambda_g = \frac{\lambda_0}{\sqrt{\varepsilon_{eff}}}$ and $\varepsilon_{eff} = \frac{\varepsilon_r+1}{2} + \frac{\varepsilon_r-1}{2}\left(\frac{1}{\sqrt{1+\left(\frac{12h}{w}\right)}} + 0.04\left(1-\left(\frac{w}{h}\right)^2\right)\right)$ Nevertheless, the comparison of the previous expressions of input impedance is not possible with one port excitation source. While, it is necessary to couple the source with the microstrip resonator, for this reason, we will introduce the technique of coupling of two port networks described by the mathematical expression which is named "Homographical relation". This technique was used by many researches[80, 81], in different forms order to correct the numerical values of input impedance given by equations(3.24) and (4.1). It may be convenient, by calculations to introduce a current source. In the first time, we need to calculate the impedance seen by the source. We are considering two surfaces, a surface S_1 which is a surface completely surrounding the source and a surface S_2 which is a section of the microstrip line oriented towards the load. Let E_1, E_2, J_1,and J_2 be the fields and currents at S_1 and S_2 as shown in Figure(4.2).

$$\begin{cases} E_2 = V_2 e_2 \\ J_2 = I_2 j_2 \end{cases} \tag{4.2}$$

Where e_2, j_2 represent respectively the fields of unitary wave. I_2 is the magnitude of J_2. The matrix impedance which relate electrical field to current density of two surfaces is given by these expressions and shown in Figure(4.9).

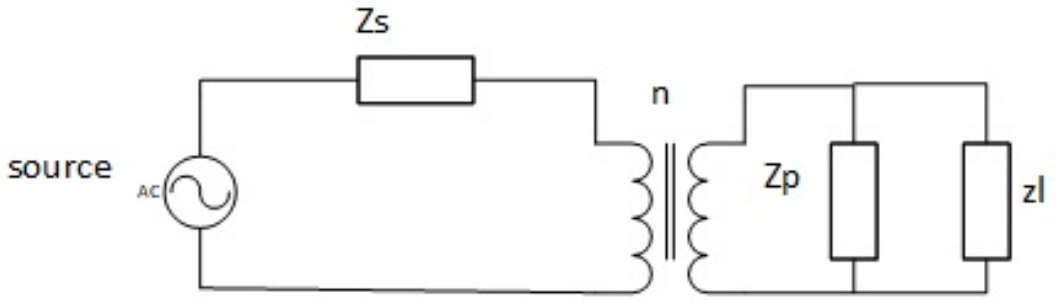

Figure 4.2: *: Equivalent Electric Circuit of Coupling*

$$E_1 = \hat{Z}_{11} J_1 + \hat{Z}_{12} j_2 I_2 \tag{4.3}$$

$$V_2 e_2 = \hat{Z}_{21} J_1 + \hat{Z}_{22} j_2 I_2 \tag{4.4}$$

We multiply the two previous equations(4.4) and (4.5) by J_1 and j_2, we can obtain the below expression:

$$\langle J_1 E_1 \rangle = \left\langle J_1 \hat{Z}_{11} J_1 \right\rangle I_1 + I_2 \left\langle J_1 \hat{Z}_{12} j_2 \right\rangle \tag{4.5}$$

$$V_2 = \left\langle j_2 \hat{Z}_{21} J_1 \right\rangle I_1 + I_2 \left\langle j_2 \hat{Z}_{22} j_2 \right\rangle \tag{4.6}$$

From the value of J_1, we can evaluate the magnitude I_1 and by the next we can calculate the I_2 magnitude which equal to:

$$I_2 = \frac{\left\langle j_2 \hat{Z}_{21} J_1 \right\rangle}{z_l - \left\langle j_2 \hat{Z}_{22} j_2 \right\rangle} \tag{4.7}$$

The aim is not to calculate the matrix impedance but to deduce existence of an homographical relation between input impedance Z_{in} and load impedance z_l which given by:$z_l = \frac{V_2}{I_2}$. While the electric equation is defined these two equations:

$$V_1 = Z_{11} I_1 + Z_{12} I_2 \tag{4.8}$$

$$V_2 = Z_{21} I_1 + Z_{22} I_2 \tag{4.9}$$

However, the input impedance is given by the below expression:

$$Z_{in} = Z_{11} - \frac{Z_{12} Z_{21}}{z_l + Z_{22}} \tag{4.10}$$

In addition, the input impedance has another expression when we replacing the magnitude I_2 with its expression in equation(4.8), such that:

$$\langle J_1 E_1 \rangle = \left\langle J_1 \hat{Z}_{11} J_1 \right\rangle + \frac{\left\langle J_1 \hat{Z}_{12} j_2 \right\rangle \left\langle j_2 \hat{Z}_{21} J_1 \right\rangle}{z_l - \left\langle j_2 \hat{Z}_{22} j_2 \right\rangle} \tag{4.11}$$

We dividing the previous equation by $|I_1|^2$, we can obtain this new expression of input impedance given by the equation:

$$Z_{in} = \frac{\langle J_1 E_1 \rangle}{|I_1|^2} = A + \frac{B}{C z_l + 1} \tag{4.12}$$

Where A and B have the dimensions of impedance and C is without dimension. We can also express the input impedance with homographical parameters like this below equation:

$$Z_{in} = Z_s \text{in serial} \left(\frac{Z_p // z_l}{n^2} \right) \tag{4.13}$$

$$Z_{in} = Z_s + \frac{Z_p z_l}{n^2 \left(Z_p + z_l \right)} \tag{4.14}$$

Where $(Z_s, Z_p, \text{and} n)$ represent respectively the serial, parallel impedance and processing factor of equivalent electric circuit of discontinuity, which are the unknown coefficients. By identification of two equations(4.12) and (4.14), the serial impedance Z_s is equivalent to A, for parallel impedance Z_p, processing factor n, A and B will be calculated thereafter. The computation process of different coefficient is as follows: To proceed these values of Z_s, Z_p and n, we choose three different lengths $l_1 = 3\lambda_g/2$, $l_2 = 5\lambda_g/4$ and $l_3 = 11\lambda_g/8$ of short-circuited microstrip resonator given by the figure (3.10) and which are expressed with the wavelength of the waveguide. The computation proceeding was based on the Kirchoff law and given by the equation(4.15)

$$\begin{cases} l_1 = \dfrac{3\lambda_g}{2} \Rightarrow z_l = 0 \Rightarrow Z_{in_1} = \dfrac{Z_p Z_s}{Z_p + Z_s} \\ l_2 = \dfrac{5\lambda_g}{4} \Rightarrow z_l = j\infty \Rightarrow Z_{in_2} = Z_p \\ l_3 = \dfrac{11\lambda_g}{8} \Rightarrow z_l = -j \Rightarrow Z_{in_3} = \dfrac{Z_p \left(Z_s - {}^{j}/_{n^2} \right)}{Z_p + Z_s - {}^{j}/_{n^2}} \end{cases} \tag{4.15}$$

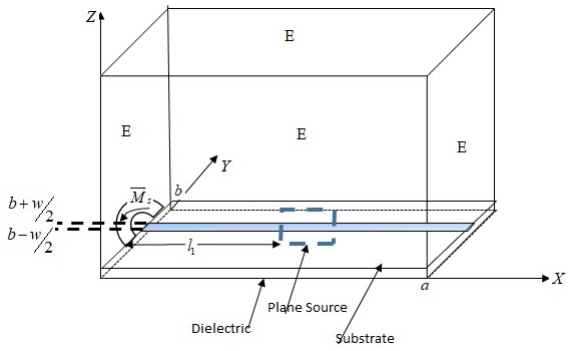

Figure 4.3: *Planar Structure Used for Homographical Relation for* $\epsilon_r = 4.4$.

4.2.2 Results Discussion

Figure(4.11) and Figure(4.12) shows the values of serial element Z_s and parallel element Z_p impedances respectively as a function of frequency variation for the two types of excitation(coaxial and planar source).

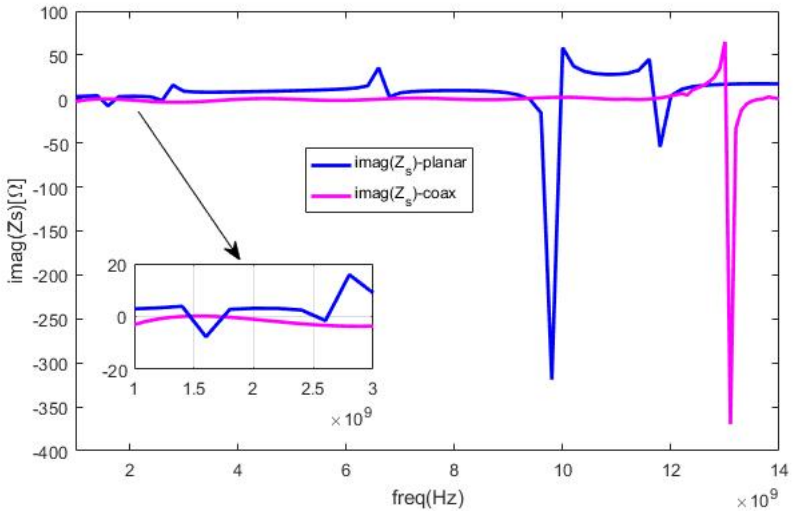

Figure 4.4: *Comparison of* Z_s *Value in Frequency Variation.*

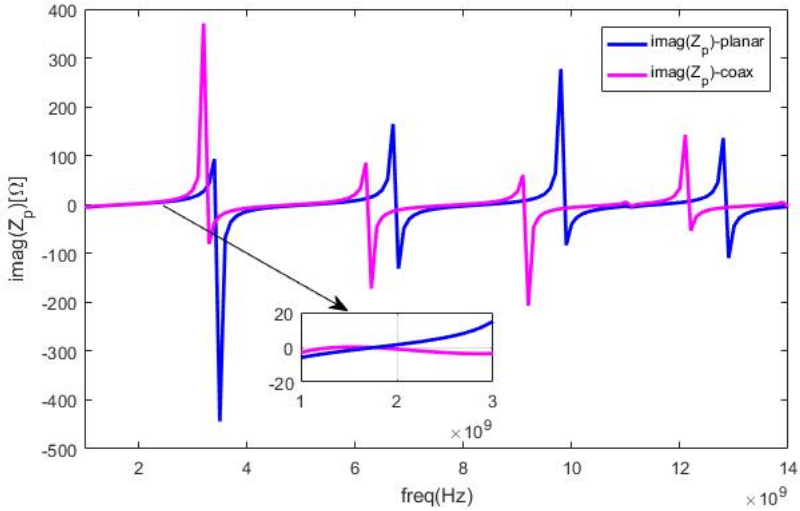

Figure 4.5: *Comparison of Z_p Value with Frequency Variation.*

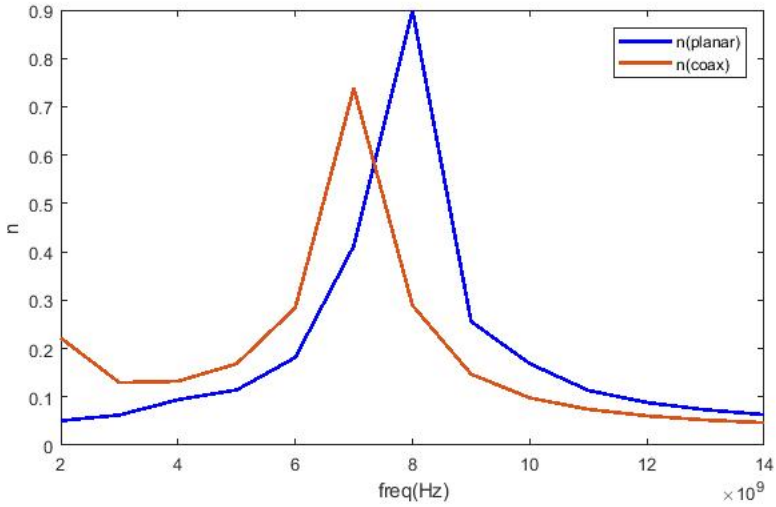

Figure 4.6: *Comparison of Processing Factor n Value with Frequency Variation for the Two Sources.*

While observing, the relative curves to Z_s and Z_p, we notice a similar behavior of serial and parallel resonance circuit with approximation between values found for both excitation: coaxial and planar, essentially for low frequencies range [1GHz to 3GHz]. The Z_s of planar source approaches from that of coaxial source. Furthermore, in this frequency range [1:3] GHz, Z_s of planar source behaves as inductance and of the coaxial source behaves as capacity. Also, in the same frequency range Z_p of coaxial source behaves like an inductance and for the planar source behaves as capacity. Where the higher order modes generated at the discontinuity are a localized type(evanescent). Same for the processing factor n Figure(4.13), we observe in the case of the two excitations considered only a good coupling between cylindrical TEM mode (or the TEM mode of planar source) of coaxial excitation and quasi-TEM mode of microstrip structure for specific frequency value which equal to $7GHz$ that could be explained by the approximation of characteristic impedance relating to this. However, in frequency equal to $9GHz$, we observe, a serial resonance in transformer primary($Z_s = 0$) and parallel resonance in secondary($Z_p = \infty$). Also, at the same frequency, the coupling value is small which bring us to resize the structure such as $\frac{h}{w} = \frac{1}{2\pi} \log\left(\frac{r_{out}}{r_{\text{in}}}\right)$ and the current value of two sources is given by:

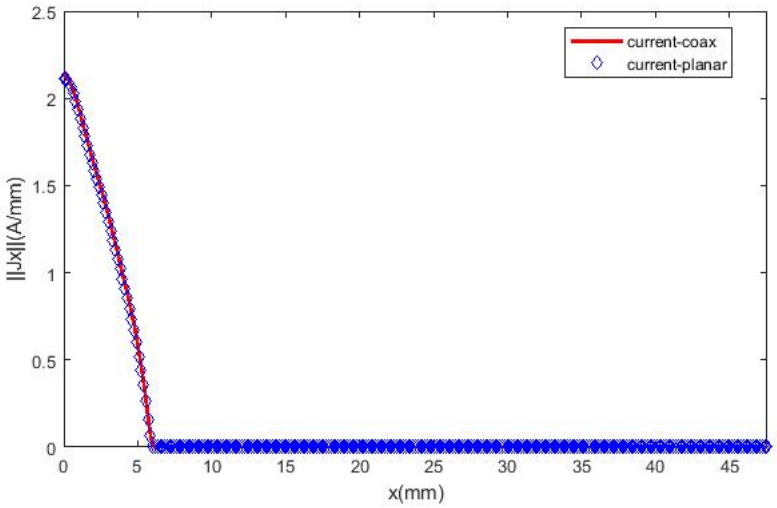

Figure 4.7: *Comparison of Current Value of Two Sources.*

In this condition that mentioned, the planar source represent the mathematical modeling of coaxial source. For getting a good model of coaxial source with that planar, it's necessary to respect planar dimensions compared to coaxial. In addition, the equivalent circuit representing the studied discontinuity for both source in given by Figure(4.8), where L_s and C_s present respectively serial inductance and capacitance,

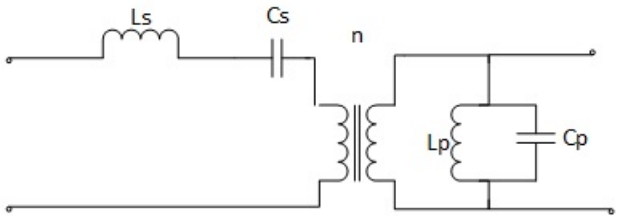

Figure 4.8: *Electric Equivalent Circuit of Discontinuity.*

L_p and C_p are respectively the parallel inductance and capacitance.

4.3 Planar Source

In this figure, we replace the coaxial source by the planar source and we will calculate the same parameters to that one cited in the previous chapter by applying the reciprocity theorem combined with MGEC. We applied the reciprocity theorem to

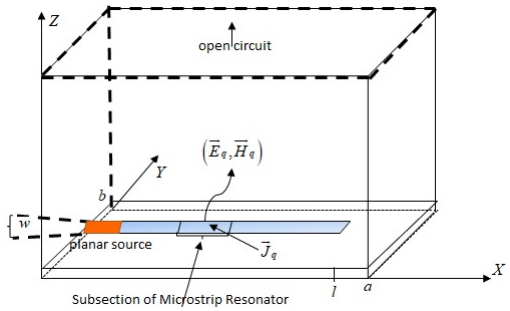

Figure 4.9: *Microstrip Resonator Excited with Planar Source sizing a=47.55mm, b=22.15mm, h=1.5mm, ϵ_r=4.32 ,freq=9GHz*

the above structure but at this time we will change coaxial source by planar source. In addition, same formulation will be obtained like that one which developed in the previous chapter but at this time the excitation vector is given by: $B = E_0 = f_0 V$. The results obtained in current, field distributions and also the input impedance value will be discussed in the next sections.

4.3.1 Study of Convergence

For reaching the convergence, we need to increase the modal functions number by fixing the test functions number. Figure(4.10) shows the study of convergence according to modal functions $M = N = 300$ and test functions $P = Q = 10$. Hence, we will consider these values to model the structure given in this work. Compared to convergence value for coaxial source cited in previous chapter, we noticed that the relationship in dimension between planar source and coaxial should be verify this condition $\frac{h}{w} = \frac{1}{2\pi} \log\left(\frac{r_{out}}{r_{\text{in}}}\right)$ at frequency equal to $9GHz$.

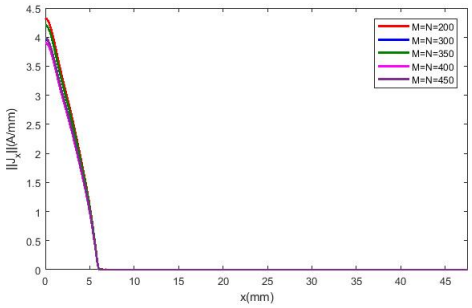

Figure 4.10: *Study of Current Convergence*

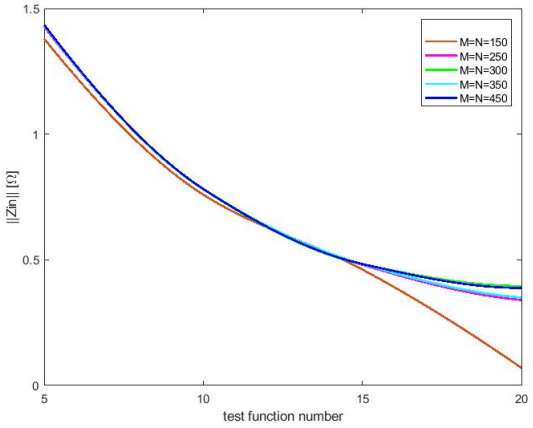

Figure 4.11: *Convergence of Impedance*

Figure(4.10) shows the convergence of current distribution of structure excited by planar source, we notice that the current keep the same behavior from $M = N = 300$ and $P = Q = 10$.

4.3.2 Current Distribution

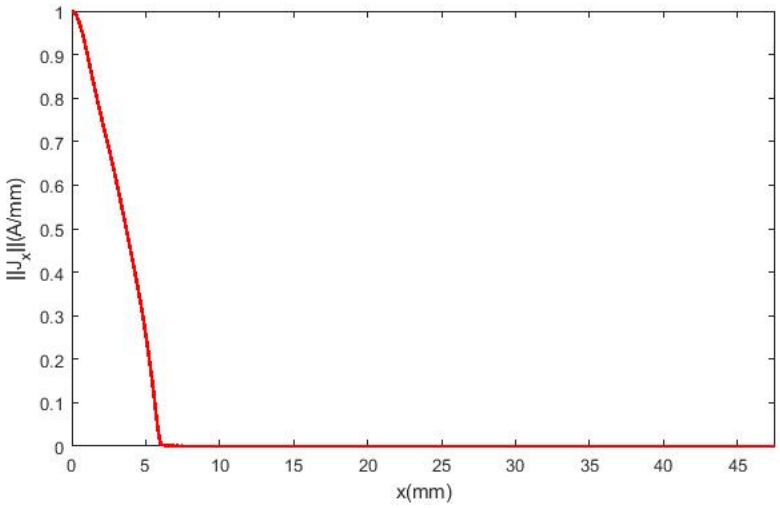

Figure 4.12: *Current Density Distribution*

4.3.3 Electric Field Distribution

In this figure, we noticed that the electric field is maximum near the excitation source and in the end of the metallic microstrip resonator. So, it verified the boundary condition of an open metallic waveguide. However, the using of virtuel waveguide didn't disturb the behavior of electric field.

4.3.4 Electric Field Distribution (yoz) plane

Figure(4.14) schematized the variation of electric field radiated in z plane of the waveguide. We noticed that for the small values of the height(z) of the waveguide, the electric field was disturbed by the evanescent mode which propagated near the discontinuity plane. Those modes gives the design antenna characteristic. If we move away from the discontinuity plane, the evanescent modes disappeared and only the propagate modes which appeared that created the far electric field ($z = \lambda_g$).

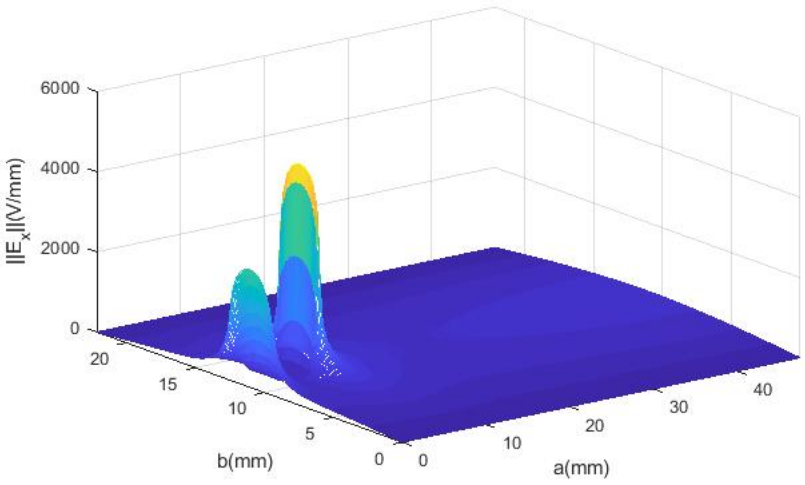

Figure 4.13: *Electric Field Distribution in* (xoy) *plane*

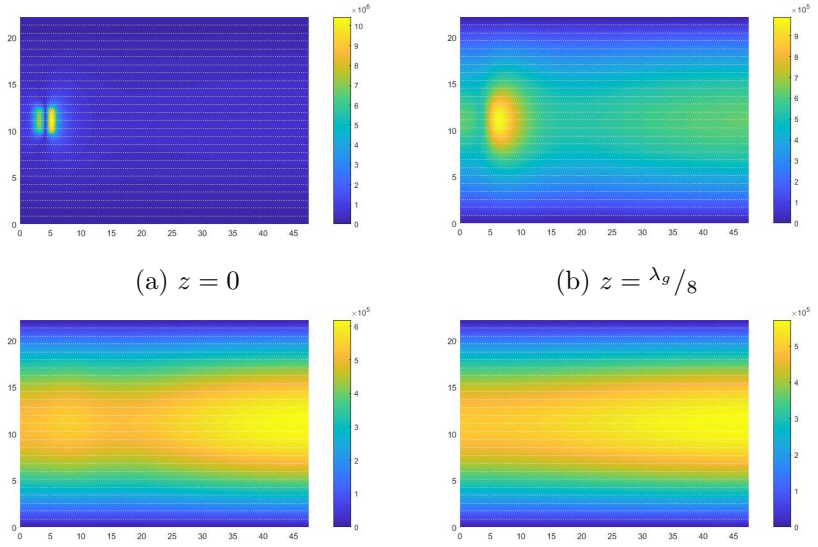

(a) $z = 0$ (b) $z = {}^{\lambda_g}/_8$

(c) $z = {}^{\lambda_g}/_3$ (d) $z = \lambda_g$

Figure 4.14: Electric Field Distribution by Varying the Height of the Waveguide

4.3.5 Value of Z_{in}

The value of input impedance Z_{in} of microstrip line excited with planar source is given by the below equation:

$$Z_{in} = \frac{\langle J_0, E \rangle}{\langle J_0, J_0 \rangle} \tag{4.16}$$

where J_0 is the current source of planar excitation and E^{tot} is the electric field in the waveguide. However, the value of input input is shows by the below figures:

1.

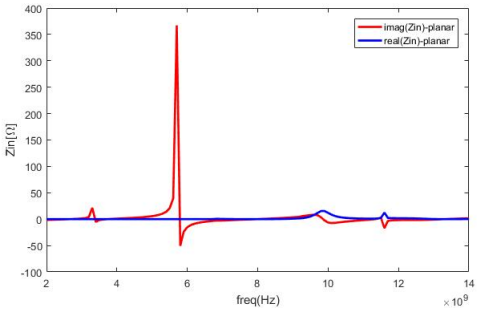

(a) *Value of Z_{in} of Planar Source*

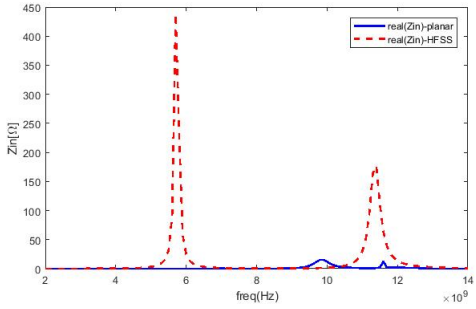

(b) *Real Part of Input Impedance with HFSS*

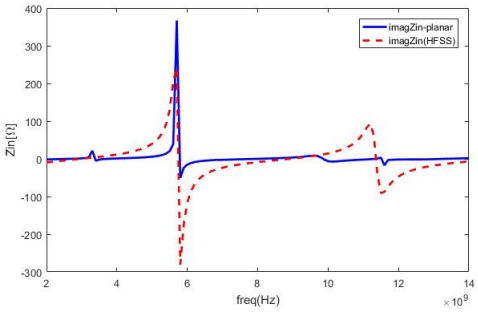

(c) *Imaginary Z_{in} of Planar Source Compared to HFSS*

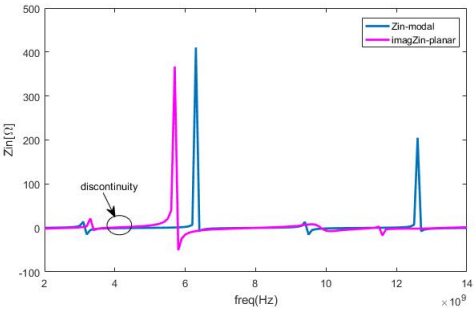

(d) *Imaginary Z_{in} Seen by Fundamental Mode*

Figure 4.15: *Value (a) of Input Impedance and Comparison of Real Part(b) and Imaginary Part Z_{in} of Microstrip Resonator Structure Excited by Planar Source with (c) HFSS and to that (d)Seen by Fundamental Mode*

Figure(4.15) gives the value of in input impedance of microstrip line resonator excited by planar source. These values of impedance are taken for microstrip resonator dimensions equal to:($l = 18.75mm$, $w = 0.31$), the length of planar source is qual to $0.5mm$ and $\epsilon_r = 2.2$. The 1st resonance frequency is equal to 5.9GHz. Compared real part and imaginary part of Zin value to HFSS simulation shown in figures (a) and (c), we found the same value. Hence, we have approximately an agreement for two different methods (reciprocity theorem combined with MGEC and FEM (Finite Element Method) for HFSS). This agreement is given also by relative error which calculated in previous chapter and given by the equation (3.23) for frequency value equal to 8.9GHz and its equal to 1.7%. But if we compare the input impedance value with the one seen by the fundamental mode (figure(d)), we found shift in frequency value. So, this prove the presence of discontinuity between planar source and microstrip resonator inside an open waveguide.
In the previous section, we are applied the reciprocity theorem on microstrip line resonator excited by the planar source. We found an agreement between resutlts obtained with our method and HFSS simulation. Hence, we are noticed the existence of discontinuity between source and structure. So, this is it will be the aim of the next section.

4.4 Conclusion

In this chapter, we applied the reciprocity theorem combined with GECM on microstrip line resonator in an open metallic waveguide excited with planar source. We found an agreement in impedance values which compared to HFSS simulation. We studied the discontinuity between planar structure and excitation (coaxial and planar) source by giving the equivalent electric circuit of discontinuity. As a conclusion, the coaxial source can be modeled by planar source.

Chapter 5

Modeling of Planar Structure Using Reciprocity Theorem Combined with MGEC

Contents

5.1 Introduction

Microstrip antennas and microstrip filters[82] are widely used in wireless communication, radar, satellite systems, and also aerospace application[83, 84]. Because of their ease manufacturing, their lightweight, low profile and also their ability to conform non-planar structure in free space. These structures need tools based on numerical techniques to be modeled and resolved some electromagnetic problems like interference, discontinuity. In this chapter, we will model a microstrip antenna with a coaxial

source in the middle. Hence, we also modeling a microstrip line filter excited from either side with coaxial cable.

5.2 Microstrip Antenna Modeling

We consider a structure given by Figure(5.1). It is described by a microstrip antenna powered by a conductor and excited by a magnetic current source existing in a coaxial aperture. This structure is located in an open-end wave guide.

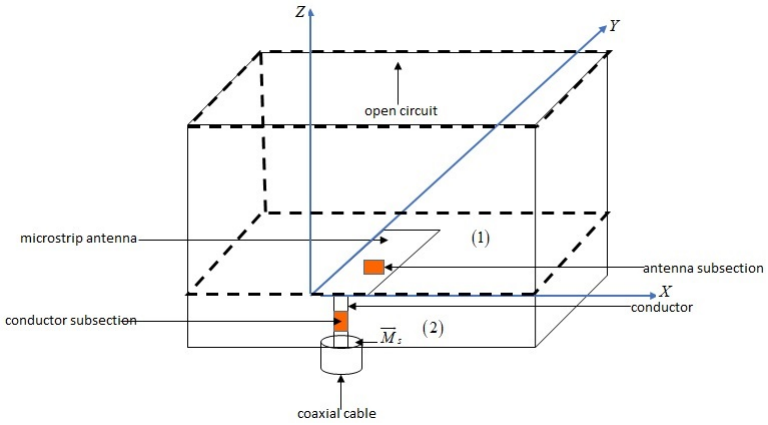

Figure 5.1: *Structure Design:* $a = 47.55mm$, $b = 22.15$, $c = 15.5mm$, $L = 24.5mm$, $W = 2.8mm$, $l = 1.5mm$, $h = 1.5mm$, $r_{in} = 0.37mm$, $r_{out} = 0.8mm$, $\epsilon_r = 1$

5.2.1 Computation of Structure Parameters

Let's consider these couple of sources $\left\{J_{s_p}, J_{q_p}, J_{s_c}, M_s, J_{qc}\right\}$ which produce these couple of electric and magnetic fields $\left\{E^t, H^t, E_q, H_q\right\}$ We applied the reciprocity theorem to the structure of Figure(5.1), we have:

$$\iiint_V \left(E^t \cdot J_q - H^t \cdot M_q - E_q \cdot J_s + H_q \cdot M_s\right) \cdot dV = 0 \tag{5.1}$$

We can write the previous equation in this form

$$\iiint_V \left(E^t \cdot J_q\right) \cdot dV = \iiint_V \left(E_q \cdot J_s - H_q \cdot M_s\right) \cdot dV \tag{5.2}$$

The first term of equation(5.2), $E^t \cdot J_q = 0$ because J_q exist in subsection of planar structure and occupied the hole volume of waveguide. Thereafter, the equation(5.2) will transform to this below equation:

$$\iiint_V \left(\overrightarrow{E}_q \cdot \overrightarrow{J}_{s_1}\right) \cdot dV + \iiint_V \left(\overrightarrow{E}_q \cdot \overrightarrow{J}_{s_2}\right) \cdot dV = \iiint_V \left(\overrightarrow{H}_q \cdot \overrightarrow{M}_s\right) \cdot dV \tag{5.3}$$

Where J_{s_1} and J_{s_2} are the distribution of current density in the microstrip antenna and in the conductor respectively. $E_q = E_{q_1} + E_{q_2}$, E_{q_1} is the auxiliary field in the microstrip antenna and E_{q_2} is that of the conductor. By application of the reciprocity theorem, we can transform the volume integral to surface integral, because the volume integral resolution is not easy to do. So, we can deduce this equation:

$$\begin{aligned} &\iint_{S_1} \left(\left(\vec{E}_{q_1} + \vec{E}_{q_2}\right)\Big|_{z=0} \cdot \vec{J}_{s_1}\right) \cdot dS_1 + \iint_{S_2} \left(\left(\vec{E}_{q_1} + \vec{E}_{q_2}\right)\Big|_{y=0} \cdot \vec{J}_{s_2}\right) \cdot dS_2 \\ &= \iint_{S_{feed}} \left(\vec{H}_{q_1} \cdot \vec{M}_s\right) .dS_{feed} + \iint_{S_{feed}} \left(\vec{H}_{q_2} \cdot \vec{M}_s\right) .dS_{feed} \end{aligned} \tag{5.4}$$

where $dS_1 = dxdy$, $dS_2 = dxdz$ and the distribution of current density of microstrip antenna and conductor are both given by the following equation

$$\begin{cases} \overrightarrow{J}_{s_1}(x,y) = x_{p_1} g_{p_1}(x,y) \cdot \overrightarrow{y} \\ \overrightarrow{J}_{s_2}(x,z) = x_{p_2} g_{p_2}(x,z) \cdot \overrightarrow{z} \end{cases} \tag{5.5}$$

The expression of the auxiliary electric field in our structure is given by the Figure(**??**):

$$\begin{cases} E_q(x,y,z) = E_{q_1}(x,y,z) + E_{q_2}(x,y,z) \\ H_q(x,y,z) = H_{q_1}(x,y,z) + H_{q_2}(x,y,z) \end{cases} \tag{5.6}$$

H_q represent the magnetic field induced by the test current J_q in the two subsections of the microstrip antenna and the conductor respectively.

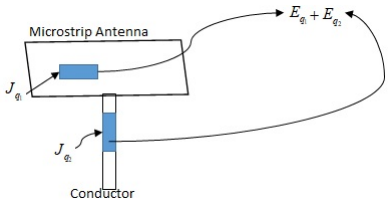

Figure 5.2: *Analyzing Structure*

The auxiliary electric field and auxiliary magnetic field which is modeled in the Figure(5.2) defined by: $E_q^{cc}(x,\, y,\, z) = \sum_n a_n f_n sh\left(\gamma_n^{cc} z\right)$: short-circuit
$E_q^{co}(x,\, y,\, z) = \sum_n a_n f_n e^{-\gamma_n^{co} z}$: open-circuit
which $a_n = z_n \langle J_q, f_n \rangle = z_n \langle I_q g_q, f_n \rangle$, g_q is the test function of each subsection and I_q represent the magnitude of J_q.

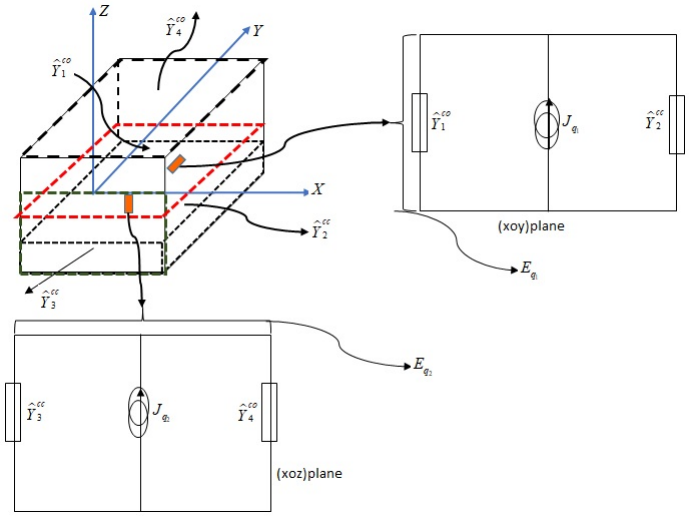

Figure 5.3: *Generalized Equivalent Circuit of Each Subsections of Microstrip Antenna Connected to Conductor*

Furthermore, the integral equation(5.6) can be written as:

$$\sum_p \underbrace{\left\langle E_{q_1}|_{z=0}, g_{p_1}\right\rangle}_{M_{11}} x_{p_1} + \sum_p \underbrace{\left\langle E_{q_2}|_{z=0}, g_{p_1}\right\rangle}_{M_{12}} x_{p_1} + \sum_p \underbrace{\left\langle E_{q_1}|_{y=0}, g_{p_2}\right\rangle}_{M_{21}} x_{p_2}$$
$$+ \sum_p \underbrace{\left\langle E_{q_2}|_{y=0}, g_{p_2}\right\rangle}_{M_{22}} x_{p_2} = \sum_q \underbrace{\left\langle \frac{j}{\omega\mu_0}\overrightarrow{rot}\left(E_{q_1}\right), M_s\right\rangle}_{A_1} + \sum_q \underbrace{\left\langle \frac{j}{\omega\mu_0}\overrightarrow{rot}\left(E_{q_2}\right), M_s\right\rangle}_{A_2} \tag{5.7}$$

We replace the auxiliary field by their expressions in equation(5.23), we can obtain the following equation:

$$\sum_p \underbrace{\langle f_n, g_{q_1}\rangle|_{z=0} z_n \langle g_{p_1}, f_n\rangle}_{M_{11}} I_{q_1} x_{p_1} + \sum_p \underbrace{\langle f_n, g_{q_2}\rangle|_{z=0} z_n \langle g_{p_1}, f_n\rangle}_{M_{21}} I_{q_2} x_{p_1}$$
$$+ \sum_p \underbrace{\langle f_n, g_{q_1}\rangle|_{y=0} z_n \langle g_{p_2}, f_n\rangle}_{M_{12}} I_{q_1} x_{p_2} + \sum_p \underbrace{\langle f_n, g_{q_2}\rangle|_{y=0} z_n \langle g_{p_2}, f_n\rangle}_{M_{22}} I_{q_2} x_{p_2}$$
$$= \sum_q \underbrace{\frac{j}{\omega\mu_0} \langle f_n g_{q_1}\rangle z_{mn} \langle rot\left(f_n\right), M_s\rangle}_{A_1} I_{q_1} + \sum_q \underbrace{\frac{j}{\omega\mu_0} \langle f_n g_{q_2}\rangle z_{mn} \langle rot\left(f_n\right), M_s\rangle}_{A_2} I_{q_2} \tag{5.8}$$

The previous equation can be transformed to matrix equation given by:

$$I_1 \left[M_{11}X_1 + M_{12}X_2 - A_1\right] + I_2 \left[M_{21}X_1 + M_{22}X_2 - A_2\right] = 0 \tag{5.9}$$

then

$$\begin{pmatrix} M_{11} & M_{12} \\ M_{21} & M_{22} \end{pmatrix} \begin{pmatrix} X_1 \\ X_2 \end{pmatrix} = \begin{pmatrix} A_1 \\ A_2 \end{pmatrix} \tag{5.10}$$

which X_1 and X_2 are the unknown vector coefficient that their values will be calculate from this equation:

$$\begin{pmatrix} X_1 \\ X_2 \end{pmatrix} = \begin{pmatrix} M_{11} & M_{12} \\ M_{21} & M_{22} \end{pmatrix}^{-1} \begin{pmatrix} A_1 \\ A_2 \end{pmatrix} \tag{5.11}$$

5.2.2 System resolution

5.2.2.1 Computation of M_{11} and M_{21} Matrix in (xoy)Plane:(Appendices D)

$M_{11} = \langle g_{p_1}, f_n\rangle\, z_n \langle f_n, g_{q_1}\rangle_{z=0}$; $M_{21} = \langle g_{p_2}, f_n\rangle\, z_n \langle f_n, g_{q_1}\rangle_{y=0}$;

5.2.2.2 Computation of M_{12} and M_{22} Matrix in (xoz)Plane:(Appendices D)

$M_{12} = \langle g_{p_2}, f_n\rangle\, z_n \langle f_n, g_{q_2}\rangle_{z=0}$; $M_{22} = \langle g_{p_2}, f_n\rangle\, z_n \langle f_n, g_{q_2}\rangle_{y=0}$

5.2.2.3 Test function in (xoy)Plane: Antenna

$$g_{q_1} = \begin{cases} 1 \; if \; x_q \leq x \leq x_{q+1} \quad \& \quad \dfrac{W - w_p}{2} \leq x \leq \dfrac{W + w_p}{2} \\ 0 \; others \end{cases} \tag{5.12}$$

$$g_{p_1} = \begin{cases} \sin\left(\dfrac{2p\pi}{L}x\right) \; if \; 0 \leq x \leq L \quad \& \quad 0 \leq y \leq W \\ 0 \; others \end{cases} \tag{5.13}$$

5.2.2.4 Test function in (xoz)Plane: Conductor

$$g_{q_2} = \begin{cases} 1 \quad if \quad z_q \leq z \leq z_{q+1} \quad \& \quad \dfrac{L - w_c}{2} \leq x \leq \dfrac{L + w_c}{2} \\ 0 \quad others \end{cases} \tag{5.14}$$

$$g_{p_2} = \begin{cases} \cos\left(\dfrac{p\pi}{l}(z + l)\right) \; if \; -l \leq z \leq 0 \; \& \; \dfrac{L - w_c}{2} \leq x \leq \dfrac{L + w_c}{2} \\ 0 \quad others \end{cases} \tag{5.15}$$

5.2.3 Results and Discussion

Figure(5.4)shows the value of the density current distribution in the conductor.

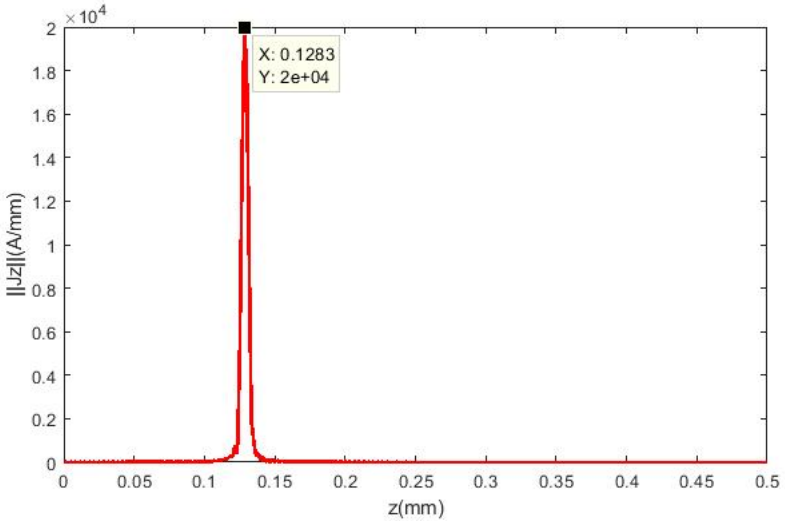

Figure 5.4: *Value of the Conductor Current Density Distribution*

We noticed that the current in conductor is maximum in the section which it was connected to the antenna. Hence, it's value verify the boundary condition which given by the conductor test function. On the other hand, the value of current density distribution in the antenna is given by the Figure(5.5).

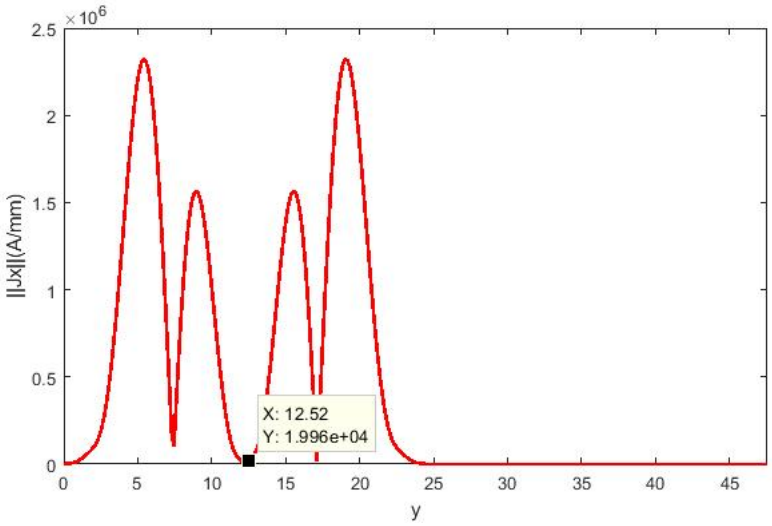

Figure 5.5: *Value of Current Density Distribution of the Antenna*

The current behavior in antenna verify the boundaries conditions of its test function. However, the value of current is taken at a frequency that equals $28GHz$ and at the same subsection width value for each element and it's equal to $0.61mm$. We noticed that the current is small in the half-length of the antenna which it's in contact with the conductor which represents its excitation source. The smallest current value is explained with the existing of the discontinuity between source and radiation element. Furthermore, the relative error between these two elements is equal to 0.4% We noticed also that the current behavior is symmetrical on both sides of the source position. The density current values of conductors and antennas are taken for test functions number is equal to $P = Q = 5$ and for that modal number is equal to $M = N = 350$. However, the variation of conductor length influences the current value. In fact, Figure(5.6) shown the variation of discontinuity value in antenna with variation of conductor length. In the first figure, the length of the conductor is equal to $2mm$, the value of discontinuity is small compared to $0.5mm$. So, if we increase or decrease the conductor length, the antenna current density value change. As a result, the antenna discontinuity affects with conductor dimensions.

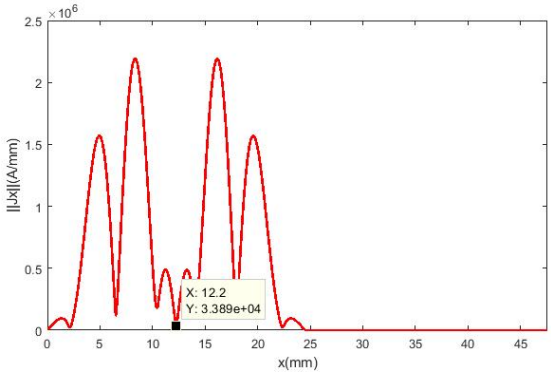

(a) *Value of Microstrip Antenna Current Density for* $l_{cond} = 2mm$

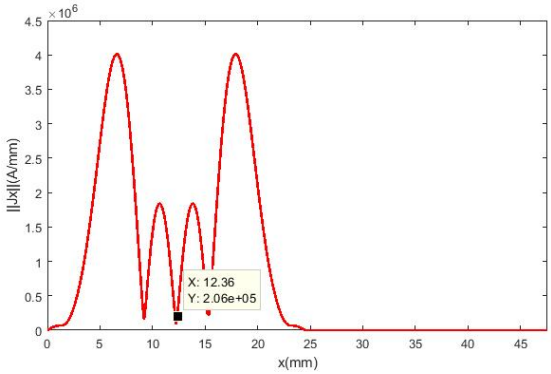

(b) *Value of Microstrip Antenna current Density for* $l_{cond} = 0.5mm$

Figure 5.6: *Value of Antenna Current Density in Conductor Length Variation*

5.3 Filter Modeling

Filter was found in many RF and microwave circuits. It existing many type of filters, for example low pass-filter which only pass signals of a low frequency range, or high pass-filter is applied to pass signals with higher frequency and block others, and also pass-band filter passes signals within a certain band of frequencies. In this context, we consider the structure which given by the following figure:

It shown two microstrip line excited by two coaxial souces and coupling by a discon-

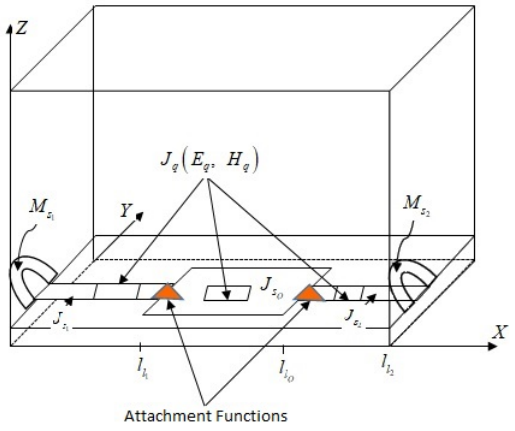

Figure 5.7: *Microstrip Filter Structure Excited by Coaxial Cable*

tinuity in the middle on the other side. A magnetic current source M_s existing in the aperture of coaxial. The current distribution density existing in the two microstrip lines also in quadruple producing the total electric field E^{tot} and the total magnetic field H^{tot} in the waveguide. An auxiliary current J_q in the subsections of microstrip lines and the discontinuity named test current produces the auxiliary electric field E_q and auxiliary magnetic field H_q. The two microstrip lines are sized by $(l_{l_1} \times w_{l_1})$ and $(l_{l_2} \times w_{l_2})$ respectively and the dimension of discontinuity is $(l_Q \times W_Q)$. However, the two microstrip lines are related to discontinuity through an attachment functions.

5.3.1 Filter Theory

By applying the reciprocity theorem to the above structure, we can deduce this mathematical relation:

$$\begin{aligned}&\iint_{S_1} E_{q_1}\cdot J_{s_1}\cdot dS_1+\iint_{S_1} E_{q_1}\cdot g_{Att_1}\cdot dS_1+\iint_{S_Q} E_{q_Q}\cdot J_{s_Q}\cdot dS_Q\\&+\iint_{S_Q} E_{q_Q}\cdot g_{Att_Q}\cdot dS_Q+\iint_{S_2} E_{q_2}\cdot J_{s_2}\cdot dS_2\\&=\iint_{S_{f_1}} H_{q_1}\cdot M_{s_1}\cdot dS_{f_1}+\iint_{S_{f_2}} H_{q_2}\cdot M_{s_2}\cdot dS_{f_2}\end{aligned}\tag{5.16}$$

where $S_1 = S_2 = (xoy)_{plane}$, $S_{f_1} = S_{f_2}(yoz)_{plane}$ of excitation source and $S_Q = (xoy)_{plane}$ surface of quadruple. We can also write the previous integral equation as a scalar product such that:

$$\left\langle E'_{q_1}, J_{s_1}\right\rangle+\left\langle E'_{q_1}, g_{Att_1}\right\rangle+\left\langle E'_{q_Q}, J_{s_Q}\right\rangle+\left\langle E'_{q_Q}, g_{Att_Q}\right\rangle+\left\langle E'_{q_2}, J_{s_2}\right\rangle=\left\langle H'_{q_1}, M_{s_1}\right\rangle+\left\langle H'_{q_2}, M_{s_2}\right\rangle\tag{5.17}$$

Applying now the reciprocity theorem combined with MGEC to the previous equation, we find the relation which gives by equation(5.1):

$$\begin{aligned}&\left\langle I_{p_1} g_{p_1}|\hat{Y}^{-1}_{1_{mn}} g_{q_1}\right\rangle+\left\langle E'_{q_1}|g_{Att_1}\right\rangle+\left\langle I_{p_Q} g_{p_Q}|\hat{Y}^{-1}_{Q_{mn}} g_{q_Q}\right\rangle+\left\langle E'_{q_Q}|g_{Att_Q}\right\rangle+\left\langle I_{p_2} g_{p_2}|\hat{Y}^{-1}_{2_{mn}} g_{q_2}\right\rangle\\&=\left\langle H'_{q_1}|M_{s_1}\right\rangle+\left\langle H'_{q_2}|M_{s_2}\right\rangle\end{aligned}\tag{5.18}$$

$\widehat{Y}_{i_{mn}}$ represent the modal admittance for each region $i = (microstrip \quad lines \quad or \quad quadruple)$. The test functions of microstrip lines g_p are defined as:

$$g_{p_1}=\begin{cases}\cos\left(\dfrac{(2p-1)\,\pi}{l_{l_1}}x\right) & if \quad 0\le x\le l_{l_1}\\ 0 \quad others\end{cases}\tag{5.19}$$

$$g_{p_2}=\begin{cases}\cos\left(\dfrac{(2p-1)\,\pi}{l_{l_2}}\left(x-(l_{l_1}+l_Q)\right)\right) & if \quad l_{l_1}+l_Q\le x\le l_{l_2}\\ 0 \quad others\end{cases}\tag{5.20}$$

The g_{p_Q} is the test function of discontinuity which given by the following equation:

$$g_{p_Q}=\begin{cases}\cos\left(\dfrac{(2p-1)\,\pi}{l_Q}\left(x-l_1\right)\right)\sin\left(\dfrac{q\pi}{W}\left(y+\dfrac{W}{2}\right)\right)\cdot\overrightarrow{x}\\ \sin\left(\dfrac{(2p+1)\,\pi}{2l_Q}\left(x-l_1\right)\right)\cos\left(\dfrac{q\pi}{W}\left(y+\dfrac{W}{2}\right)\right)\cdot\overrightarrow{y}\\ 0 \quad others\end{cases}\tag{5.21}$$

And the test function g_q for each subsection of the Figure(5.1) is defined by echelon function and it's given by:

$$g_q = \begin{cases} 1 & if \quad x_q \leq x \leq x_{q+1} \\ 0 & others \end{cases} \tag{5.22}$$

The attachment function is given by the trigonometric function:

$$g_{att} = \begin{cases} N_{att} \sin(kx - p) & if \quad x \in [l - \Delta l, l + \Delta l] \\ 0 & others \end{cases} \tag{5.23}$$

where N represent the normalization coefficient, $k = \frac{\pi}{2\Delta l}$ and $p = -k(l - \Delta l)$ are the coefficients of the attachment function.
Based on the reciprocity theorem for analyzing microstrip filter which is given by equation(5.16), the aim of this section is to give the filter parameters in reflection and transmission coefficients. However, the impedance matrix is based on the value of the input impedance of each block of our structure. Thereof, the input impedance expression is given by:

$$Z_{in} = \frac{\langle M_s, H \rangle}{\langle H, H \rangle} \tag{5.24}$$

Where the total magnetic field H has this expression:

$$H = \frac{j}{\omega \mu_0} rot(E) \tag{5.25}$$

which inspired from total electric field E^{tot} via Maxwell-Ampere relation, and

$$E = \widehat{Y}^{-1} J_s \tag{5.26}$$

by application of the method of Generalized equivalent circuit(MGEC). To obtain the value of S parameter matrix, we need to calculate the values of unknown coefficients given by the previous equations.

5.3.2 System Resolution

Since the complexity of our structure given by Figure(5.1) and the difficulty in system equations resolution , we tried to simplify our analytical computation. In addition, we are divided our structure into 3 parts: the first one is described by microstrip line open-circuit, the second one is given by the quadruple and the last one define by the microstrip line short-circuit. The system resolution wil be as follows:

- We given the input impedance value of microstrip line open-circuit as well as that of short-circuit,

- We calculated the resulting impedance matrix of the two microstrip lines,

$$Z_{lines} = \begin{bmatrix} \frac{Z_{in_{cc}}+Z_{in_{co}}}{2} & \frac{Z_{in_{cc}}-Z_{in_{co}}}{2} \\ \frac{Z_{in_{cc}}-Z_{in_{co}}}{2} & \frac{Z_{in_{cc}}+Z_{in_{co}}}{2} \end{bmatrix} = \begin{bmatrix} Z_{11_l} & Z_{12_l} \\ Z_{21_l} & Z_{22_l} \end{bmatrix} \tag{5.27}$$

- We given the impedance matrix value of the discontinuity,
- We calculated the transfer matrix of each component(two microstrip lines and discontinuity),
- We calculated the global transfer matrix of our structure,
- We given the scattering matrix from the transfer matrix,
- Finally, we given the reflection and transmitter coefficient of the microstrip filter.

5.3.2.1 Transfer Matrix and Scattering Matrix of Microstrip Filter

Impedance matrix and Transfer matrix are often used in the analysis of linear dynamical system[85] noted T. In addition the transfer matrix of two microstrip lines is given from their impedance matrix and it defined by the flowing equation:

$$T_l = \begin{bmatrix} \frac{Z_{11_l}}{Z_{21_l}} & Z_{12_l} - \frac{Z_{11_l}Z_{22_l}}{Z_{21_l}} \\ \frac{1}{Z_{22_l}} & -\frac{Z_{22_l}}{Z_{22_l}} \end{bmatrix} \tag{5.28}$$

and that of the discontinuity is written as:

$$T_Q = \begin{bmatrix} \frac{Z_{11_Q}}{Z_{21_Q}} & Z_{12_Q} - \frac{Z_{11_Q}Z_{22_Q}}{Z_{21_Q}} \\ \frac{1}{Z_{22_Q}} & -\frac{Z_{22_Q}}{Z_{22_Q}} \end{bmatrix} \tag{5.29}$$

the global transfer matrix of the microstrip filter is given by:

$$T = [T_l] \cdot [T_Q] \cdot [T_l] \tag{5.30}$$

Consequently, the scattering matrix of our structure is expressed by this equation:

$$S^{filter} = \begin{bmatrix} -\frac{T_{21}}{T_{22}} & \frac{1}{T_{22}} \\ T_{11} - \frac{T_{12}T_{21}}{T_{22}} & \frac{T_{12}}{T_{22}} \end{bmatrix} \tag{5.31}$$

5.4 Conclusion

In this chapter, We modeled a microstrip antenna in 3D space connected to a conductor in the middle and which excited by a coaxial cable. The results obtained of current density distribution in radiation element and coaxial source showed the existing of discontinuity. We noticed also from the current antenna graphs that the length of conductor affects antenna behavior. We have also developed the analytical formulation based on the Reciprocity theorem combined with MGEC techniques to model a microstrip filter for 5G applications that we will give its type in the future works.

Chapter 6

Conclusion and Future Work

In this final chapter, we summarize our work in Section 6.1 and present our future research directions in Section 6.2.

6.1 Conclusion

Our research aims is to analyze the planar discontinuity founded between excitation source which described by coaxial cable and circuit in 3-D space. This analysis has been done by an application of a volume integral method based on the reciprocity theorem which combined with MGEC. Besides, we have started by giving the discontinuity problems in microwave domain and resolution techniques used in this context especially in 3-d space. We are concentrated on the numerical methods in their integral form especially based on the method of moment(MOM). We are shown from much research that the method of moment is unable to resolve planar discontinuity in 3-D. We are an integral technique derived from the method of moment and which car resolve volumetric discontinuity. This technique named the "Reciprocity Theorem". After that, we have applied this technique combined with the MGEC on the planar structure described by microstrip resonator in an open-end metallic waveguide which excited with a coaxial source. Furthermore, in this chapter, we are concentrated on the development of coaxial source excitation formulation. The results obtained in the density of current and field distribution verified the boundaries conditions of the metallic waveguide. The value of input impedance obtained shows an agreement with HFSS simulations also with measurement results. Compared this one to that found by fundamental mode, We observed a discontinuity which studied in the next chapter. Consequently, in this chapter, we studied the discontinuity that exists between the source and planar structure. A homographical relation was written in the function of input impedance. Results obtained in serial parameter and parallel parameter and also in coupling value proven that the planar source represent the mathematical model of coaxial in this condition $\frac{h}{w} = \frac{1}{2\pi} \log\left(\frac{r_{out}}{r_{\text{in}}}\right)$ and for this frequency $9GHz$. Hence, we are given the characteristic in the current, the electrical and the impedance of the planar source. Finally, we applied this hybridization to model two structures, the

first one is described by microstrip antenna excited by coaxial cable vias a conductor. We concluded that the conductor length effects on antenna current behavior. The second one is described with a microstrip filter in that, we given our mathematical formulation.

6.2 Future Work

The study of planar discontinuity in 3D space with real source possessed some difficulties in mathematical resolution and the big computational time. In this context, we resort to find or to implement an optimization algorithm which can minimize CPU computational time. Also, we try to apply this apply in industrial millimeter-wave applications. Hence, the theory of a microstrip filter that developed in the last chapter in our manuscript will be implemented in 5G application which will study and given its type for fifth-generation frequency.

Appendices

Appendix A

Modal Functions Definition

The modal functions of metallic waveguide EEEE
TE modal :

$$TE_{mn} = \begin{vmatrix} \frac{\frac{n}{b}}{\sqrt{\left(\frac{m}{a}\right)^2 + \left(\frac{n}{b}\right)^2}} \sqrt{\frac{4}{ab}} \cos\left(K_x x\right) \sin\left(K_y y\right) \\ \frac{-\frac{m}{a}}{\sqrt{\left(\frac{m}{a}\right)^2 + \left(\frac{n}{b}\right)^2}} \sqrt{\frac{4}{ab}} \sin\left(K_x x\right) \cos\left(K_y y\right) \end{vmatrix}$$

$$TE_{0n} = \begin{vmatrix} \sqrt{\frac{2}{ab}} \sin\left(K_y y\right) \\ 0 \end{vmatrix} \text{ and } TE_{m0} = \begin{vmatrix} 0 \\ -\sqrt{\frac{2}{ab}} \sin\left(K_x x\right) \end{vmatrix}$$

TM modal:

$$TM_{mn} = \begin{vmatrix} \frac{-\frac{m}{a}}{\sqrt{\left(\frac{m}{a}\right)^2 + \left(\frac{n}{b}\right)^2}} \sqrt{\frac{4}{ab}} \cos\left(K_x x\right) \sin\left(K_y y\right) \\ \frac{\frac{n}{b}}{\sqrt{\left(\frac{m}{a}\right)^2 + \left(\frac{n}{b}\right)^2}} \sqrt{\frac{4}{ab}} \sin\left(K_x x\right) \cos\left(K_y y\right) \end{vmatrix}$$

TM_{0n} and TM_{m0} not exist.

Appendix B

Microstrip Resonator Formulation

B.1 Structure Description

Using the structure of Figure(3.1) and Figure(3.5) of chapter(3). Based on the reciprocity theorem combined with MGEC, we can find this expression

$$\iiint_V \left(\overrightarrow{E}^{tot} \cdot \overrightarrow{J}_q\right) \cdot dV = \iiint_V \left(\overrightarrow{E}_q \cdot \overrightarrow{J_S} - \overrightarrow{H}_q \cdot \overrightarrow{M}_S\right) \cdot dV \tag{B.1}$$

By applying the reciprocity theorem, we can transform the volume integral to surface as following:

$$\iint_{S_{strip}} \left(\vec{E}_q\left(z=0\right) \cdot \vec{J}_S\right) \cdot dS = \iint_{S_{feed}} \left(\vec{M}_S \cdot \vec{H}_q\left(x=0\right)\right) \cdot dS \tag{B.2}$$

If we multiply the equation(3.12) by the coefficient I_q, we will find the following equation:

$$I_q\left[\langle g_p, E_q\left(z=0\right)\rangle\right] \cdot \left[I_p\right] = I_q\left[\langle M_s, H_q\left(x=0\right)\rangle\right] \tag{B.3}$$

which can be written as:

$$\left[\left\langle g_p, E_q^{'}\left(z=0\right)\right\rangle\right] \cdot \left[I_p\right] = \left[\left\langle M_s, H_q^{'}\left(x=0\right)\right\rangle\right] \tag{B.4}$$

where $E_q^{'} = I_q E_q$ and $H_q^{'} = I_q H_q$

B.2 System Resolution

B.2.1 Value of A Matrix

$$\begin{aligned} A &= \left[\left\langle g_p\left(x,y\right), E_q^{'}\left(z=0\right)\right\rangle\right] = \left[\left\langle g_p\left(x,y\right), \hat{Y}^{-1} \cdot g_q\left(x\right)\right\rangle\right] \\ &= \left[\left\langle g_p\left(x,y\right), \hat{Z}_{mn} \cdot g_q\left(x\right)\right\rangle\right] \end{aligned} \tag{B.5}$$

where g_p and g_q are the test function respectively of the microstrip resonator and of the subsection which defined in chapter(3).

B.2.2 Modal Admittance Expression

The modal admittance $\hat{Y}_1$ and $\hat{Y}_2$ used in equation(B.5) are given by: $\hat{Y}_1 = \sum_{\substack{m,n \\ \alpha=TE,TM}} |f^{\alpha}_{mn}\rangle Y^{\alpha}_{1mn} \langle f^{\alpha}_{mn}|$ and $\hat{Y}_2 = \sum_{\substack{m,n \\ \alpha=TE,TM}} |f^{\alpha}_{mn}\rangle Y^{\alpha}_{2mn} \langle f^{\alpha}_{mn}|$

The analytic expressions of modal functions $(f^{\alpha}_{mn})_{m,n\in TE,TM}$ are given in appendix A. The modal admittance $(Y^{\alpha}_{1mn})_{\substack{m,n\in N \\ \alpha=TE,TM}}$ and $(Y^{\alpha}_{2mn})_{\substack{m,n\in N \\ \alpha=TE,TM}}$ given the waveguide behavior: short or open circuit.

Modal Admittance of an open-end waveguide:

$$Y^{TE}_{1vmn} = \frac{\gamma^{TE}_{1vmn}}{j\omega\mu_0} \tag{B.6}$$

where $\gamma_{1mn} = \sqrt{K_x^2 + K_y^2 - K_0^2}$

$$Y^{TM}_{1vmn} = \frac{j\omega\varepsilon_0}{\gamma_{1vmn}} \tag{B.7}$$

Modal Admittance of a short circuit waveguide:

$$Y^{TE}_{2hmn} = \frac{\gamma^{TE}_{2hmn}}{j\omega\mu_0} coth\left(\gamma_{2hmn}h\right) \tag{B.8}$$

where $\gamma_{2mn} = \sqrt{K_x^2 + K_y^2 - K_0^2\varepsilon_r}$

$$Y^{TM}_{2hmn} = \frac{j\omega\varepsilon}{\gamma_{2hmn}} coth\left(\gamma_{2hmn}h\right) \tag{B.9}$$

The modal impedance is given by: $z^{\alpha}_{mn} = {}^{1}/_{y^{\alpha}_{mn}}$

TE_{mn} modal(Appendix A)

$$\begin{aligned} A_{TE_{mn}} &= \sum_{p,q}\sum_{m,n} \left\langle g_p(x,y), \left(\left|f^{TE}_{mn}\right\rangle z_{mn} \left\langle f^{TE}_{mn}\right| \cdot g_q(x,y)\right)\right\rangle \\ &= \sum_{p,q}\sum_{m,n} \underbrace{\left\langle g_p(x,y), f^{TE}_{mn}\right\rangle}_{1} z_{mn} \underbrace{\left\langle f^{TE}_{mn}, g_q(x,y)\right\rangle}_{2} \end{aligned} \tag{B.10}$$

x projection of modal functions:

$$\begin{aligned}
A_{TE_{mn}} &= \sum_{p,q}\sum_{m,n}\iint g_p(x,y)\cdot f_{mn}^{TE}dxdy \\
&= \sum_{p,q}\sum_{m,n}\frac{\frac{n}{b}}{\sqrt{\left(\frac{m}{a}\right)^2+\left(\frac{n}{b}\right)^2}}\sqrt{\frac{4}{ab}}\iint g_p(x,y)\cos(K_x x)\sin(K_y y)dxdy \\
&= \sum_{p,q}\sum_{m,n}\frac{\frac{n}{b}}{\sqrt{\left(\frac{m}{a}\right)^2+\left(\frac{n}{b}\right)^2}}\sqrt{\frac{4}{ab}}\int_0^l\int_{\frac{b-w}{2}}^{\frac{b+w}{2}} g_p(x,y)\cos(K_x x)\sin(K_y y)\,dxdy \\
&\cdot\frac{\frac{n}{b}}{\sqrt{\left(\frac{m}{a}\right)^2+\left(\frac{n}{b}\right)^2}}\sqrt{\frac{4}{ab}}\int_{x_q}^{x_{q+1}}dx\int_{\frac{b-w}{2}}^{\frac{b+w}{2}}dy
\end{aligned} \tag{B.11}$$

Finally the value of A matrix for TE is

$$\begin{aligned}
A_{TE_{mn}} = \sum_{p,q}\sum_{m,n} &\left[\frac{\frac{n}{b}}{\sqrt{\left(\frac{m}{a}\right)^2+\left(\frac{n}{b}\right)^2}}\sqrt{\frac{4}{ab}}\right]^2\cdot\left[\frac{\cos\left(K_y\frac{b-w}{2}\right)-\cos\left(K_y\frac{b-w}{2}\right)}{K_y}\right]^2\cdot\left[\frac{\sin(K_x x_q)-\sin(K_x x_{q+1})}{K_x}\right] \\
&\cdot\frac{1}{2}\left[\frac{\sin\left(\left(K_x+\frac{(2p-1)\pi}{2L}\right)l\right)}{K_x+\frac{(2p-1)\pi}{2l}}+\frac{\sin\left(\left(K_x-\frac{(2p-1)\pi}{2l}\right)l\right)}{K_x-\frac{(2p-1)\pi}{2l}}\right]
\end{aligned} \tag{B.12}$$

TM modal form

$$\begin{aligned}
A_{TM_{mn}} = \sum_{p,q}\sum_{m,n} &\left[\frac{-\frac{m}{a}}{\sqrt{\left(\frac{m}{a}\right)^2+\left(\frac{n}{b}\right)^2}}\sqrt{\frac{4}{ab}}\right]^2\cdot\left[\frac{\cos\left(K_y\frac{b-w}{2}\right)-\cos\left(K_y\frac{b-w}{2}\right)}{K_y}\right]^2\cdot\left[\frac{\sin(K_x x_q)-\sin(K_x x_{q+1})}{K_x}\right] \\
&\cdot\frac{1}{2}\left[\frac{\sin\left(\left(K_x+\frac{(2p-1)\pi}{2l}\right)l\right)}{K_x+\frac{(2p-1)\pi}{2l}}+\frac{\sin\left(\left(K_x-\frac{(2p-1)\pi}{2L}\right)l\right)}{K_x-\frac{(2p-1)\pi}{2l}}\right]
\end{aligned} \tag{B.13}$$

The next step will give the value of I_p which given by $I_p=\frac{B}{A}$. Replacing A and B by their expressions, we will find the value of unknown coefficient I_p.

Appendix C

Coaxial Source

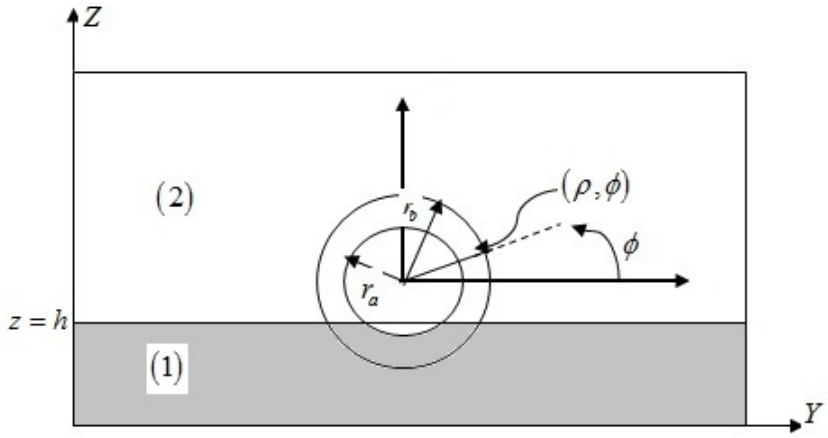

Figure C.1: *Coaxial Source.*

We have two excitation source coaxial and planar source. In this section, we will give a detailed computation of coaxial source. Figure(C.1) described the coaxial structure, which r_a and r_b are respectively the inner and outer radius of coaxial. Our excitation is defined by equation(3.18), the magnetic current source is given by equation(3.15) and the magnetic field is defined by equation(3.10)in chapter(3). We notice that the electric field $E_q^{'}$ is equal to $I_q \cdot E_q$ and also the magnetic field $H_q^{'}$ is equal to $I_q \cdot H_q$ as announced in appendix B. Thereof,the electrical field $E_q^{'}$ in region(2)is expressed by:

$$\overrightarrow{E}_q^{\prime(2)} = \begin{cases} \sum_{mn}^{TE,TM} \underbrace{\langle f_{mnx}, g_q \rangle}_{\alpha_{mnq}} y_{mn}^{-1} f_{mnx} e^{-\gamma_{mn}^{(2)} z} \cdot \overrightarrow{x} \\ \sum_{mn}^{TE,TM} \underbrace{\langle f_{mny}, g_q \rangle}_{\alpha_{mnq}} y_{mn}^{-1} f_{mny} e^{-\gamma_{mn}^{(2)} z} \cdot \overrightarrow{y} \\ 0 \end{cases} \tag{C.1}$$

and the field $E_q^{'}$ in region(1)is given by the following equation:

$$\overrightarrow{E}_q^{'(1)} = \begin{cases} \sum_{mn}^{TE,TM} \underbrace{\langle f_{mnx}, g_q \rangle}_{\alpha_{mnq}} y_{mn}^{-1} f_{mnx} sh\left(\gamma_{mn}^{(1)}(z+l_1)\right) \cdot \overrightarrow{x} \\ \sum_{mn}^{TE,TM} \underbrace{\langle f_{mny}, g_q \rangle}_{\alpha_{mnq}} y_{mn}^{-1} f_{mny} sh\left(\gamma_{mn}^{(1)}(z+l_1)\right) \cdot \overrightarrow{y} \\ 0 \end{cases} \tag{C.2}$$

Where f_{mn} represent the modal function of TE and TM modes of waveguide covered with electric walls, $g_q$is the test function in microstrip resonator subsection defined by echelon, γ_{mn} represent waveguide propagation,for region(2) is defined by:

$$\gamma_{mn}^{(2)} = \sqrt{\left(\frac{m\pi}{a}\right)^2 + \left(\frac{n\pi}{b}\right)^2 - K_0^2} \tag{C.3}$$

for region(1)is given by:

$$\gamma_{mn}^{(1)} = \sqrt{\left(\frac{m\pi}{a}\right)^2 + \left(\frac{n\pi}{b}\right)^2 - K_0^2 \varepsilon_{r_1}} \tag{C.4}$$

From the value of $E_q^{'}$ we can give the value of $H_q^{'}$ of region(2) which equal to:

$$\begin{cases} H_{q_x}^{'}(x\,|=0) = 0 \\ H_{q_y}^{'}(x\,|=0) = \sum_{mn,q}^{TE,TM} -\frac{j\alpha_{mnq}^{TE,TM}}{\omega\mu_0} \gamma_{mn}^{I(TE,TM)} coef_x^{TE,TM} \cdot \\ \qquad e^{-\gamma_{mn}^{(2)(TE,TM)} z} \sin(K_y y)\, y_{mn}^{-1} \\ H_{q_z}^{'}(x\,|=0) = \sum_{mn,q}^{TE,TM} \frac{j\alpha_{mnq}^{TE,TM}}{\omega\mu_0} \begin{bmatrix} K_x coef_y^{TE,TM} - \\ K_y coef_x^{TE,TM} \end{bmatrix} \cdot \\ \qquad e^{-\gamma_{mn}^{(2)(TE,TM)} z} \cos(K_y y)\, y_{mn}^{-1} \end{cases} \tag{C.5}$$

where $K_x = \frac{m\pi}{a}$ and $K_y = \frac{n\pi}{b}$, a and b represent respectively length and width of waveguide, $coef_x = \frac{\frac{n}{b}}{\sqrt{\left(\frac{m}{a}\right)^2 + \left(\frac{n}{b}\right)^2}} \sqrt{\frac{4}{ab}}$ and $coef_y = \frac{-\frac{m}{a}}{\sqrt{\left(\frac{m}{a}\right)^2 + \left(\frac{n}{b}\right)^2}} \sqrt{\frac{4}{ab}}$. The last value of excitation vector is given by the below equation:

$$\begin{aligned} V_q &= \sum_q \left\langle (M_{sy} + M_{sz}), \left(H_{qy}^{'} + H_{qz}^{'}\right) \right\rangle_i \\ &= \sum_q \left\langle M_{sy}, H_{qy}^{'} \right\rangle_i + \sum_q \left\langle M_{sz}, H_{qz}^{'} \right\rangle_i \end{aligned} \tag{C.6}$$

where $i = region(1,2)$ of the source. The source excitation vector will be calculated for all propagation modes.

Variable Relation	Vector Relation
$x = x$	$\widehat{x} = \widehat{x}$
$y = \rho \cos(\phi)$	$\widehat{y} = \cos(\phi)\,\hat{\rho} - \sin(\phi)\,\hat{\phi}$
$z = \rho \sin(\phi)$	$\widehat{z} = \sin(\phi)\,\hat{\rho} + \cos(\phi)\,\hat{\phi}$

Table C.1: *Transformation Variables Coordinates*

Appendix D

Microstrip Antenna Element Matrix

D.1 Computation of Modal Function in (xoy) Plane: EEEE Wall

f_{mn}^{TE} modal function of short-circuit case:

$$f_{mn}^{TE}(x,y,z=0)=\begin{vmatrix}\frac{\frac{n}{b}}{\sqrt{\left(\frac{m}{a}\right)^2+\left(\frac{n}{b}\right)^2}}\sqrt{\frac{4}{ab}}\cos(K_x x)\sin(K_y y)\,sh(\gamma_{mn}^{cc}z)\\ \frac{-\frac{m}{a}}{\sqrt{\left(\frac{m}{a}\right)^2+\left(\frac{n}{b}\right)^2}}\sqrt{\frac{4}{ab}}\sin(K_x x)\cos(K_y y)\,sh(\gamma_{mn}^{cc}z)\end{vmatrix}=0 \quad (D.1)$$

$coef_x=\frac{\frac{n}{b}}{\sqrt{\left(\frac{m}{a}\right)^2+\left(\frac{n}{b}\right)^2}}\sqrt{\frac{4}{ab}}$; $coef_y=\frac{\frac{-m}{a}}{\sqrt{\left(\frac{m}{a}\right)^2+\left(\frac{n}{b}\right)^2}}\sqrt{\frac{4}{ab}}$

$f_{0n}^{TE}$and f_{m0}^{TE} modal of short-circuit case:

$$f_{0n}^{TE}(x,y,z=0)=\begin{vmatrix}\sqrt{\frac{2}{ab}}\sin(K_y y)\,sh(\gamma_{0n}^{cc}z)\\ 0\end{vmatrix}=0 \quad (D.2)$$

$$f_{m0}^{TE}(x,y,z=0)=\begin{vmatrix}0\\ -\sqrt{\frac{2}{ab}}\sin(k_x x)\,sh(\gamma_{m0}^{cc}z)\end{vmatrix}=0 \quad (D.3)$$

f_{mn}^{TM}modal of short-circuit case:

$$f_{mn}^{TM}(x,y,z=0)=\begin{vmatrix}\frac{-\frac{m}{a}}{\sqrt{\left(\frac{m}{a}\right)^2+\left(\frac{n}{b}\right)^2}}\sqrt{\frac{4}{ab}}\cos(k_x x)\sin(k_y y)\,sh(\gamma_{mn}^{cc}z)\\ \frac{\frac{n}{b}}{\sqrt{\left(\frac{m}{a}\right)^2+\left(\frac{n}{b}\right)^2}}\sqrt{\frac{4}{ab}}\sin(k_x x)\cos(k_y y)\,sh(\gamma_{mn}^{cc}z)\end{vmatrix}=0 \quad (D.4)$$

$\underline{f_{mn}^{TE} \text{ modal of open-circuit case:}}$

$$\begin{aligned} f_{mn}^{TE}(x,y,z=0) &= \begin{vmatrix} \frac{\frac{n}{b}}{\sqrt{\left(\frac{m}{a}\right)^2+\left(\frac{n}{b}\right)^2}}\sqrt{\frac{4}{ab}}\cos(k_x x)\sin(k_y y)\, e^{-(\gamma_{mn}^{co} z)} \\ \frac{-\frac{m}{a}}{\sqrt{\left(\frac{m}{a}\right)^2+\left(\frac{n}{b}\right)^2}}\sqrt{\frac{4}{ab}}\sin(k_x x)\cos(k_y y)\, e^{-(\gamma_{mn}^{co} z)} \end{vmatrix} \\ &= \begin{vmatrix} \frac{\frac{n}{b}}{\sqrt{\left(\frac{m}{a}\right)^2+\left(\frac{n}{b}\right)^2}}\sqrt{\frac{4}{ab}}\cos(k_x x)\sin(k_y y) \\ \frac{-\frac{m}{a}}{\sqrt{\left(\frac{m}{a}\right)^2+\left(\frac{n}{b}\right)^2}}\sqrt{\frac{4}{ab}}\sin(k_x x)\cos(k_y y) \end{vmatrix} \end{aligned} \tag{D.5}$$

$\underline{f_{0n}^{TE} \text{and } f_{m0}^{TE} \text{ modal of open-circuit case:}}$

$$\begin{aligned} f_{0n}^{TE}(x,y,z=0) &= \begin{vmatrix} \sqrt{\frac{2}{ab}}\sin(k_y y)\, e^{-(\gamma_{mn}^{co} z)} \\ 0 \end{vmatrix} \\ &= \begin{vmatrix} \sqrt{\frac{2}{ab}}\sin(k_y y) \\ 0 \end{vmatrix} \end{aligned} \tag{D.6}$$

$$\begin{aligned} f_{m0}^{TE}(x,y,z=0) &= \begin{vmatrix} 0 \\ -\sqrt{\frac{2}{ab}}\sin(K_x x)\, e^{-(\gamma_{mn}^{co} z)} \end{vmatrix} \\ &= \begin{vmatrix} 0 \\ -\sqrt{\frac{2}{ab}}\sin(K_x x) \end{vmatrix} \end{aligned} \tag{D.7}$$

$\underline{f_{mn}^{TM} \text{ modal of open-circuit case:}}$

$$f_{mn}^{TM}(x,y,z=0) = \begin{vmatrix} \frac{-\frac{m}{a}}{\sqrt{\left(\frac{m}{a}\right)^2+\left(\frac{n}{b}\right)^2}}\sqrt{\frac{4}{ab}}\cos(k_x x)\sin(k_y y)\, e^{-(\gamma_{mn}^{co} z)} \\ \frac{\frac{n}{b}}{\sqrt{\left(\frac{m}{a}\right)^2+\left(\frac{n}{b}\right)^2}}\sqrt{\frac{4}{ab}}\sin(k_x x)\cos(k_y y)\, e^{-(\gamma_{mn}^{co} z)} \end{vmatrix}$$
$$= \begin{vmatrix} \frac{-\frac{m}{a}}{\sqrt{\left(\frac{m}{a}\right)^2+\left(\frac{n}{b}\right)^2}}\sqrt{\frac{4}{ab}}\cos(k_x x)\sin(k_y y) \\ \frac{\frac{n}{b}}{\sqrt{\left(\frac{m}{a}\right)^2+\left(\frac{n}{b}\right)^2}}\sqrt{\frac{4}{ab}}\sin(k_x x)\cos(k_y y) \end{vmatrix} \tag{D.8}$$

D.2 Computation of Modal Functions in (xoz) Plane: EEEE Walls

$\underline{f_{mn}^{TE} \text{ modal function of short-circuit case:}}$

$$f_{mn}^{TE}(x,y=0,z) = \begin{vmatrix} 0 \\ \frac{-\frac{m}{a}}{\sqrt{\left(\frac{m}{a}\right)^2+\left(\frac{n}{b}\right)^2}}\sqrt{\frac{4}{ab}}\sin(k_x x)\, sh(\gamma_{mn}^{cc} z) \end{vmatrix} \tag{D.9}$$

$\underline{f_{0n}^{TE} \text{and } f_{m0}^{TE} \text{ modal of short-circuit case:}}$

$$f_{0n}^{TE}(x,y=0,z) = \begin{vmatrix} 0 \\ 0 \end{vmatrix} \tag{D.10}$$

$$f_{m0}^{TE}(x,y=0,z) = \begin{vmatrix} 0 \\ -\sqrt{\frac{2}{ab}}\sin(k_x x)\, sh(\gamma_{m0}^{cc} z) \end{vmatrix} \tag{D.11}$$

$\underline{f_{mn}^{TM} \text{modal of short-circuit case:}}$

$$f_{mn}^{TM}(x,y=0,z) = \begin{vmatrix} 0 \\ \frac{\frac{n}{b}}{\sqrt{\left(\frac{m}{a}\right)^2+\left(\frac{n}{b}\right)^2}}\sqrt{\frac{4}{ab}}\sin(k_x x)\, sh(\gamma_{mn}^{cc} z) \end{vmatrix} \tag{D.12}$$

f_{mn}^{TE} modal of open-circuit case:

$$f_{mn}^{TE}(x, y=0, z) = \begin{vmatrix} 0 \\ \frac{-\frac{m}{a}}{\sqrt{\left(\frac{m}{a}\right)^2 + \left(\frac{n}{b}\right)^2}} \sqrt{\frac{4}{ab}} \sin(k_x x)\, e^{-(\gamma_{mn}^{co} z)} \end{vmatrix} \tag{D.13}$$

$f_{0n}^{TE}$and f_{m0}^{TE} modal of open-circuit case:

$$f_{0n}^{TE}(x, y=0, z) = \begin{vmatrix} 0 \\ 0 \end{vmatrix} \tag{D.14}$$

$$f_{m0}^{TE}(x, y=0, z) = \begin{vmatrix} 0 \\ -\sqrt{\frac{2}{ab}} \sin(k_x x)\, e^{-(\gamma_{mn}^{co} z)} \end{vmatrix} \tag{D.15}$$

f_{mn}^{TM} modal of open-circuit case:

$$f_{mn}^{TM}(x, y=0, z) = \begin{vmatrix} 0 \\ \frac{\frac{n}{b}}{\sqrt{\left(\frac{m}{a}\right)^2 + \left(\frac{n}{b}\right)^2}} \sqrt{\frac{4}{ab}} \sin(k_x x)\, e^{-(\gamma_{mn}^{co} z)} \end{vmatrix} \tag{D.16}$$

TM_{m0} and TM_{0n} modals not exists

D.3 Computation of the Sub-Matrix Elements

D.3.1 Short Circuit Waveguide

$$\begin{aligned} M_{11} &= \sum_{p,q,n} \langle g_{p_1}, f_n \rangle \cdot z_n \cdot \langle f_n, g_{q_1} \rangle_{z=0} \cdot sh(\gamma_n^{cc} z) \\ &= \sum_{p,q,n} coef_y^2 \int_0^L \int_{\frac{a-W}{2}}^{\frac{a+W}{2}} g_{p_1} \cdot f_n dxdy \cdot z_n \cdot \int_{y_q}^{y_{q+1}} \int_{\frac{a-W}{2}}^{\frac{a+W}{2}} f_n \cdot g_{q_1} \cdot sh(\gamma_n^{cc} z)\, dxdy = 0 \end{aligned} \tag{D.17}$$

$$\begin{aligned} M_{12} &= \sum_{p,q,n} \langle g_{p_1}, f_n \rangle \cdot z_n \cdot \langle f_n, g_{q_2} \rangle|_{z=0} \cdot sh(\gamma_n^{cc} z) \\ &= \sum_{p,q,n} coef_y^2 \int_0^L \int_{\frac{a-W}{2}}^{\frac{a+W}{2}} g_{p_1} \cdot f_n dxdy \cdot z_n \cdot \int_{y_q}^{y_{q+1}} \int_{\frac{W-w_c}{2}}^{\frac{W+w_c}{2}} f_n \cdot g_{q_2} \cdot sh(\gamma_n^{cc} z) dxdy = 0 \end{aligned} \tag{D.18}$$

$$M_{21} = \sum_{p,q,n} \langle g_{p_2}, f_n \rangle \cdot z_n \cdot \langle f_n, g_{q_1} \rangle|_{y=0} \cdot sh\left(\gamma_n^{cc} z\right)$$

$$= \sum_{p,q,n} coef_y^2 \int_{-h}^{0} \int_{\frac{W-w_c}{2}}^{\frac{W+w_c}{2}} g_{p_2} \cdot f_n dxdz \cdot z_n \int_{z_q}^{z_{q+1}} \int_{0}^{\frac{W+w_c}{2}} f_n \cdot g_{q_1} \cdot sh\left(\gamma_n^{cc} z\right) dxdz$$

$$= \sum_{p,q,n} coef_y^2 \cdot \int_{-h}^{0} \int_{\frac{W-w_c}{2}}^{\frac{W+w_c}{2}} \cos\left(\frac{p\pi\left(z+h\right)}{h}\right) \sin\left(K_x x\right) dxdz \cdot z_n \cdot \int_{z_q}^{z_{q+1}} \int_{0}^{\frac{W+w_c}{2}} \sin\left(K_x x\right) \cdot g_{q_1} \cdot sh\left(\gamma_n^{cc} z\right) dxdz \tag{D.19}$$

$$M_{22} = \sum_{p,q,n} \langle g_{p_2}, f_n \rangle \cdot z_n \cdot \langle f_n, g_{q_2} \rangle|_{y=0} \cdot sh\left(\gamma_n^{cc} z\right)$$

$$= \sum_{p,q,n} coef_y^2 \int_{-h}^{0} \int_{\frac{W-w_c}{2}}^{\frac{W+w_c}{2}} g_{p_2} \cdot f_n dxdz \cdot z_n \int_{z_q}^{z_{q+1}} \int_{\frac{W-w_c}{2}}^{\frac{W+w_c}{2}} f_n \cdot g_{q_2} \cdot sh\left(\gamma_n^{cc} z\right) dxdz$$

$$= \sum_{p,q,n} coef_y^2 \int_{-h}^{0} \int_{\frac{W-w_c}{2}}^{\frac{W+w_c}{2}} \cos\left(\frac{p\pi\left(z+h\right)}{h}\right) \cdot \sin\left(K_x x\right) dxdz \cdot z_n \cdot \int_{z_q}^{z_{q+1}} \int_{\frac{W-w_c}{2}}^{\frac{W+w_c}{2}} \sin\left(K_x x\right) \cdot g_{q_2} \cdot sh\left(\gamma_n^{cc} z\right) dxdz \tag{D.20}$$

D.3.2 Open Circuit Waveguide

$$M_{11} = \sum_{p,q,n} \langle g_{p_1}, f_n \rangle \cdot z_n \cdot \langle f_n, g_{q_1} \rangle_{z=0} e^{(-\gamma_n^{co} z)}$$

$$= \sum_{p,q,n} coef_y^2 \cdot \int_{0}^{L} \int_{\frac{a-W}{2}}^{\frac{a+W}{2}} g_{p_1} \cdot f_n dxdy \cdot z_n \cdot \int_{y_q}^{y_{q+1}} \int_{\frac{a-W}{2}}^{\frac{a+W}{2}} f_n \cdot g_{q_1} dxdy$$

$$= \sum_{p,q,n} coef_y^2 \cdot \int_{0}^{L} \int_{\frac{a-W}{2}}^{\frac{a+W}{2}} \cos\left(\frac{p\pi}{2L} y\right) \cdot \sin\left(K_x x\right) \cdot \cos\left(K_y y\right) dxdy \cdot z_n \cdot \int_{y_q}^{y_{q+1}} \int_{\frac{a-W}{2}}^{\frac{a+W}{2}} \sin\left(K_x x\right) \cdot \cos\left(K_y y\right) \cdot g_{q_1} dxdy \tag{D.21}$$

$$M_{12} = \sum_{p,q,n} \langle g_{p_1}, f_n \rangle \cdot z_n \cdot \langle f_n, g_{q_2} \rangle_{z=0} \cdot e^{(-\gamma_n^{co} z)}$$

$$= \sum_{p,q,n} coef_y^2 \cdot \int_{0}^{L} \int_{\frac{a-W}{2}}^{\frac{a+W}{2}} \cos\left(\frac{p\pi}{2L} y\right) \cdot \sin\left(K_x x\right) \cos\left(K_y y\right) dxdy \cdot z_n \cdot \int_{y_q}^{y_{q+1}} \int_{-\frac{w_c}{2}}^{\frac{w_c}{2}} \sin\left(K_x x\right) \cos\left(K_y y\right) \cdot g_{q_2} dxdy \tag{D.22}$$

$$M_{21} = \sum_{p,q,n} \langle g_{p_2}, f_n \rangle \, z_n \, \langle f_n, g_{q_1} \rangle|_{y=0} e^{(-\gamma_n^{co} z)}$$

$$= \sum_{p,q,n} coef_y^2 \cdot \int_{-h}^{0} \int_{-\frac{w_c}{2}}^{\frac{w_c}{2}} g_{p_2} \cdot f_n dx dz \cdot z_n \cdot \int_{z_q}^{z_{q+1}} \int_{\frac{W-w_c}{2}}^{\frac{W-w_c}{2}} f_n \cdot g_{q_1} \cdot e^{(-\gamma_n^{co} z)} dx dz$$

$$= \sum_{p,q,n} coef_y^2 \cdot \int_{-h}^{0} \int_{-\frac{w_c}{2}}^{\frac{w_c}{2}} \cos\left(\frac{p\pi\,(z+h)}{h}\right) \cdot \sin\left(K_x x\right) dx dz \cdot z_n \cdot \int_{z_q}^{z_{q+1}} \int_{\frac{W-w_c}{2}}^{\frac{W+w_c}{2}} \sin\left(K_x x\right) \cdot g_{q_1} \cdot e^{(-\gamma_n^{co} z)} dx dz \tag{D.23}$$

$$M_{22} = \sum_{p,q,n} \langle g_{p_2}, f_n \rangle \cdot z_n \cdot \langle f_n, g_{q_2} \rangle|_{y=0} \cdot e^{(-\gamma_n^{co} z)}$$

$$= \sum_{p,q,n} \int_{-h}^{0} \int_{-\frac{w_c}{2}}^{\frac{w_c}{2}} g_{p_2} \cdot f_n dx dz \cdot z_n \int_{z_q}^{z_{q+1}} \int_{-\frac{w_c}{2}}^{\frac{w_c}{2}} f_n \cdot g_{q_2} \cdot e^{(-\gamma_n^{co} z)} dx dz$$

$$= \sum_{p,q,n} coef_y^2 \cdot \int_{-h}^{0} \int_{-\frac{w_c}{2}}^{\frac{w_c}{2}} \cos\left(\frac{p\pi\,(z+h)}{h}\right) \cdot \sin\left(K_x x\right) dx dz \cdot z_n \cdot \int_{z_q}^{z_{q+1}} \int_{-\frac{w_c}{2}}^{\frac{w_c}{2}} \sin\left(K_x x\right) \cdot g_{q_2} \cdot e^{(-\gamma_n^{co} z)} dx dz \tag{D.24}$$

The previous equations will be resolved by using these trigonometric functions:
$\cos(a)\cos(b) = \frac{\cos(a+b)+\cos(a-b)}{2}$;
$\cos(a)\sin(b) = \frac{\sin(a+b)-\sin(a-b)}{2}$;
$\exp(x) = ch(x) - sh(x) = \cos(x) - i\sin(x)$;
$ch(x) = \cos(ix)$;
$sh(x) = \frac{1}{i}\sin(ix) = -i\sin(ix)$;
$\cos(x + k\pi) = \pm\cos(x)$;
$\sin(x + k\pi) = \pm\sin(x)$ with $k \in \Re$
$\cos(x + iy) = \cos(x)\,ch(y) - i\sin(x)\,sh(y)$;
$\sin(x + iy) = \sin(x)\,ch(y) + i\,s\,h(x)\cos(y)$

D.3.3 Computation of Sub-Vector Elements

$$A_{11_{att}} = \sum_{q} \left\langle E_{q_1|z=0}, g_{att_1} \right\rangle = \sum_{q,n} a_{1_n} \left\langle f_{n|z=0}, g_{att_1} \right\rangle \tag{D.25}$$

$$A_{12_{att}} = \sum_{q} \left\langle E_{q_2|z=0}, g_{att_1} \right\rangle = \sum_{q,n} a_{2_n} \left\langle f_{n|z=0}, g_{att_1} \right\rangle \tag{D.26}$$

$$A_{21} = \sum_{q} \left\langle E_{q_1|y=0}, g_{att_2} \right\rangle = \sum_{q,n} a_{1_n} \left\langle f_{n|y=0}, g_{att_2} \right\rangle \tag{D.27}$$

$$A_{22} = \sum_{q} \left\langle E_{q_2|y=0}, g_{att_2} \right\rangle = \sum_{q,n} a_{2_n} \left\langle f_{n|y=0}, g_{att_2} \right\rangle \tag{D.28}$$

Appendix E

List of Publications

1. Raja Mchaalia, Mourad Aidi and Taoufik Aguili, *A New 3D MOM-GEC Formulation Based on Reciprocity Theorem: Analysis of The Dipole Antenna*, International Conference ACES (indexed IEEE), August 1 -4, 2017.

2. Raja Mchaalia, Bilel Hamdi and Taoufik Aguili, *Reciprocity Theorem-MGEC Combined with Floquet Model Analysis to Model 5G Application*, 5G & SC Days, Tunisia, February 28 - March 3, 2019.

3. Raje Mchaalia, Mourad Aidi and Taoufik Aguili, *Study of Planar Structure Applying Reciprocity Technique Combined with MGEC and Analysis of Discontinuity*, International Journal of RF and Microwave Computer-Aided Engineering, acceptance, 2019-05-10.

Bibliography

[1] Janet Golio and Mike Golio. *RF and microwave passive and active technologies*. CRC press, 2007.

[2] R Timothy Hitchcock. *Radio-frequency and microwave radiation*. AIHA, 2004.

[3] Graham A Jones, David H Layer, and Thomas G Osenkowsky. *National Association of Broadcasters Engineering Handbook: NAB Engineering Handbook*. Taylor & Francis, 2013.

[4] *Radio‐Frequency and Microwave Communication Circuits*. John Wiley & Sons, Ltd, 1 edition, 2004.

[5] Bumper Sticker. Aps news apsnews. *THE AMERICAN PHYSICAL SOCIETY*, 7(4), 1998.

[6] Ms Neha Sharma, Sachin Chawla, and Taruna Sikha. Performance comparison of (2tx1r) and (2tx2r) mimo cdma system using space time block code (stbc).

[7] Garrison C Cavell. *National Association of Broadcasters Engineering Handbook*. Routledge, 2017.

[8] JANET GOLIOl MIKE GOLIO. *WHAT ARE MİCROWAVE?* LIVE SCIENCE CONTRIBUTOR, FEBRUARY 8,2018.

[9] National Research Council et al. Committee on microwave processing of materials: An emerging industrial technology. *Microwave processing of materials*, 1994.

[10] David M Pozar. *Microwave engineering*. John Wiley & Sons, 2009.

[11] Richard J Cameron, Chandra M Kudsia, and Raafat R Mansour. *Microwave filters for communication systems: fundamentals, design, and applications*. John Wiley & Sons, 2018.

[12] David M Pozar. Microwave engineering. *Wiley*, 2012.

[13] Robert E Collin. Field theory of guided waves. 1960.

[14] VH Rumsey. Reaction concept in electromagnetic theory. *Physical Review*, 94(6):1483, 1954.

[15] Rajeev Bansal. *Fundamentals of engineering electromagnetics*. CRC press, 2018.

[16] Essam S Tony and Sujeet K Chaudhuri. Analysis of shielded lossy multilayered-substrate microstrip discontinuities. *IEEE Transactions on Microwave Theory and Techniques*, 49(4):701–711, 2001.

[17] Maurice I Sancer, Kubilay Sertel, John L Volakis, and Peter Van Alstine. On volume integral equations. *IEEE transactions on antennas and propagation*, 54(5):1488–1495, 2006.

[18] T-S Horng, William E McKinzie, and Nicolaos G Alexopoulos. Full-wave spectral-domain analysis of compensation of microstrip discontinuities using triangular subdomain functions. *IEEE transactions on microwave theory and techniques*, 40(12):2137–2147, 1992.

[19] David B Davidson. *Computational electromagnetics for RF and microwave engineering*. Cambridge University Press, 2010.

[20] Bao Zhu, Jiefu Chen, Wanxie Zhong, and QH Liu. A hybrid finite-element/finite-difference method with an implicit–explicit time-stepping scheme for maxwell's equations. *International Journal of Numerical Modelling: Electronic Networks, Devices and Fields*, 25(5-6):607–620, 2012.

[21] Mériam Attia. *Contribution de l'approche fréquentielle de la méthode TLM dans la modélisation des dispositifs en hyperfréquences*. PhD thesis, Télécom Bretagne; Université de Bretagne Occidentale, 2012.

[22] Andrzej Demenko and Jan K Sykulski. Analogies between finite-difference and finite-element methods for scalar and vector potential formulations in magnetic field calculations. *IEEE Transactions on Magnetics*, 52(6):1–6, 2016.

[23] E Newman and D Pozar. Electromagnetic modeling of composite wire and surface geometries. *IEEE Transactions on Antennas and Propagation*, 26(6):784–789, 1978.

[24] Ramesh Garg. *Analytical and computational methods in electromagnetics*. Artech house, 2008.

[25] Roger F Harrington. *Time-harmonic electromagnetic fields*. McGraw-Hill, 1961.

[26] Raja Mchaalia, Mourad Aidi, and Taoufik Aguili. A new 3d mom-gec formulation based on reciprocity theorem: Analysis of the dipole antenna. In *2017 International Applied Computational Electromagnetics Society Symposium (ACES)*, pages 1–2. IEEE, 2017.

[27] MS Neiman. The principle of reciprocity in antenna theory. *Proceedings of the IRE*, 31(12):666–671, 1943.

[28] Ehab Salahat, Ahmed Kulaib, Nazar Ali, and Raed Shubair. Exploring symmetry in wireless propagation channels. In *2017 European Conference on Networks and Communications (EuCNC)*, pages 1–6. IEEE, 2017.

[29] ESSAM E Hassan. Field solution, polarization, and eigenmodes of shielded microstrip transmission line. *IEEE transactions on microwave theory and techniques*, 34(8):845–852, 1986.

[30] Juan M Rius, Rafael Pous, and Angel Cardama. Integral formulation of the measured equation of invariance: A novel sparse matrix boundary element method. *IEEE transactions on magnetics*, 32(3):962–967, 1996.

[31] Chokri Boussetta, Fabien Ndagijimana, Jean Chilo, and Pierre Saguet. A general methodology of modelling 3d discontinuities using the tlm method. In *1994 24th European Microwave Conference*, volume 2, pages 1524–1529. IEEE, 1994.

[32] Thomas Becks and Ingo Wolff. Analysis of 3-d metallization structures by a full-wave spectral domain technique. *IEEE TRANSACTIONS ON MICROWAVE THEORY AND TECHNIQUES*, 40(12):2219–2227, DECEMBER 1992.

[33] Wolfgang JR Hoefer. The transmission-line matrix method-theory and applications. *IEEE Transactions on Microwave Theory and Techniques*, 33(10):882–893, 1985.

[34] Rakesh Chadha and KC Gupta. Compensation of discontinuities in planar transmission lines. *IEEE Transactions on Microwave Theory and Techniques*, 30(12):2151–2156, 1982.

[35] T-S Horng, S-C Wu, H-Y Yang, and NG Alexopoulos. A generalized method for distinguishing between radiation and surface-wave losses in microstrip discontinuities. *IEEE Transactions on Microwave Theory and Techniques*, 38(12):1800–1807, 1990.

[36] Michael Arthur Thorburn. Analysis and modeling of discontinuities and interelement coupling in passive microwave integrated circuit components. 1991.

[37] Virag V Chaware, Jean-Jacques DeLisle, Jeffrey T Kemp, Noah P Montena, Ryan D Vaughan, Murat Ozbas, Joseph F Revelli, and Robert J Bowman. Experimental verification of a passive sensing node for monitoring rf connector-coaxial cable system performance. *IEEE Sensors Journal*, 14(6):1754–1764, 2014.

[38] Levent Sevgi. Reciprocity: some remarks from a field point of view. *IEEE Antennas and Propagation Magazine*, 52(2):205–210, 2010.

[39] J Richmond. A reaction theorem and its application to antenna impedance calculations. *IRE Transactions on Antennas and Propagation*, 9(6):515–520, 1961.

[40] Yin Sun, Bin-Chyi Tseng, Hank Lin, and Chulsoon Hwang. Rfi noise source quantification based on reciprocity. In *2018 IEEE Symposium on Electromagnetic*

Compatibility, Signal Integrity and Power Integrity (EMC, SI & PI), pages 548–553. IEEE, 2018.

[41] Stuart Ballantine. Reciprocity in electromagnetic, mechanical, acoustical, and interconnected systems. *Proceedings of the Institute of Radio Engineers*, 17(6):927–951, 1929.

[42] John R Carson. The reciprocal energy theorem. *Bell System Technical Journal*, 9(2):325–331, 1930.

[43] Paul Poincelot. Le théorème de réciprocite de l'électromagnétisme théorique. In *Annales des Télécommunications*, volume 16, pages 154–162. Springer, 1961.

[44] Jurgen Kunisch. Implications of lorentz reciprocity for ultra-wideband antennas. In *2007 IEEE International Conference on Ultra-Wideband*, pages 214–219. IEEE, 2007.

[45] Jasper J Goedbloed. Reciprocity and emc measurements. *TIJDSCHRIFT-NERG*, 71(1):15, 2006.

[46] DAVIDM Pozar. A reciprocity method of analysis for printed slot and slot-coupled microstrip antennas. *IEEE Transactions on Antennas and Propagation*, 34(12):1439–1446, 1986.

[47] Haradhan Mohajan. Analysis of reciprocity and substitution theorems, and slutsky equation. 2017.

[48] W Welch. Reciprocity theorems for electromagnetic fields whose time dependence is arbitrary. *IRE Transactions on Antennas and Propagation*, 8(1):68–73, 1960.

[49] W Welch. Comments on" reciprocity theorems for electromagnetic fields whose time dependence is arbitrary". *IRE Transactions on Antennas and Propagation*, 9(1):114–115, 1961.

[50] Adrianus T de Hoop. Time-domain reciprocity theorems for electromagnetic fields in dispersive media. *Radio science*, 22(7):1171–1178, 1987.

[51] B Cheo. A reciprocity theorem for electromagnetic fields with general time dependence. *IEEE Transactions on Antennas and Propagation*, 13(2):278–284, 1965.

[52] Martin Stumpf. *Electromagnetic reciprocity in antenna theory*. John Wiley & Sons, 2017.

[53] Glenn S Smith. A direct derivation of a single-antenna reciprocity relation for the time domain. *IEEE Transactions on Antennas and Propagation*, 52(6):1568–1577, 2004.

[54] Ping Li, Yifei Shi, Li Jun Jiang, and Hakan Bağcı. A dgtd scheme for modeling the radiated emission from duts in shielding enclosures using near electric field only. *IEEE Transactions on Electromagnetic Compatibility*, 58(2):457–467, 2016.

[55] Liang Li, Jingnan Pan, Chulsoon Hwang, Gyuyeong Cho, Harkbyeong Park, Yaojiang Zhang, and Jun Fan. Radio-frequency interference estimation by reciprocity theorem with noise source characterized by huygens's equivalent model. In *2016 IEEE International Symposium on Electromagnetic Compatibility (EMC)*, pages 358–363. IEEE, 2016.

[56] Rene AC Baelemans, Adrian T Sutinjo, Peter J Hall, A Bart Smolders, Michel J Arts, and Eloy de Lera Acedo. Closed-form jones matrix of dual-polarized inverted-vee dipole antennas over lossy ground. *IEEE Transactions on Antennas and Propagation*, 65(1):26–35, 2016.

[57] Chao Yang, Jiancheng Shi, Qinhuo Liu, and Yang Du. Scattering from inhomogeneous dielectric cylinders with finite length. *IEEE Transactions on Geoscience and Remote Sensing*, 54(8):4555–4569, 2016.

[58] Liang Li, Jingnan Pan, Chulsoon Hwang, Gyuyeong Cho, Harkbyeong Park, Yaojiang Zhang, and Jun Fan. Measurement validation for radio-frequency interference estimation by reciprocity theorem. In *2015 IEEE International Symposium on Electromagnetic Compatibility (EMC)*, pages 154–159. IEEE, 2015.

[59] Eleni A Lekka, Konstantinos D Paschaloudis, and George A Kyriacou. Phased array design for near field focused hyperthermia based on reciprocity theorem. In *2017 International Workshop on Antenna Technology: Small Antennas, Innovative Structures, and Applications (iWAT)*, pages 277–280. IEEE, 2017.

[60] Jose A Martinez-Lorenzo, Antonio G Pino, Javier Gutierrez, Borja G Valdes, Marcos A Acuna, Oscar Rubinos, and Fernando Las-Heras. Reflector antenna analysis using the complex equivalent length concept: Reciprocity and coupling between feeds. *IEEE Antennas and Propagation Magazine*, 51(4):88–96, 2009.

[61] Jack H Richmond. On the variational aspects of the moment method (electromagnetics). *IEEE transactions on Antennas and Propagation*, 39(4):473–479, 1991.

[62] Walton C Gibson. *The method of moments in electromagnetics*. Chapman and Hall/CRC, 2007.

[63] Roger F Harrington. Matrix methods for field problems. *Proceedings of the IEEE*, 55(2):136–149, 1967.

[64] Nejla Oueslati and Taoufik Aguili. New implementation of the moment method based on the impedance operator to study the dispersion characteristics of

microstrip lines. *International Journal of Computer Science Issues (IJCSI)*, 11(5):59, 2014.

[65] T Aguili. Modélisation des composants sh f planaires par la méthode des circuits équivalents généralisés. *Thesis Manuscript, National Engineering School of Tunis, Tunisia*, 2000.

[66] Dorsaf Omri, Mourad Aidi, and Taoufik Aguili. Transient response of coupled wire antennas using the electric field integral equation with laguerre polynomials as temporal basis functions. In *2014 IEEE International Conference on Ultra-WideBand (ICUWB)*, pages 245–250. IEEE, 2014.

[67] K Grayaa, T Aguili, and A Bouallegue. Integrating genetic algorithm with mom analysis for planar microstrip structures. *Journal of Microwaves, Optoelectronics and Electromagnetic Applications (JMOe)*, 5(2):101–110, 2006.

[68] Mourad Aidi. *Modélisation Électromagnétique Des Antennes Miniatures à Base de Nanotubes de Carbone et de Graphène Dans la Bande Térahertz*. PhD thesis, Ecole Nationale d'Ingénieurs de Tunis, 2016.

[69] Sonia Mili, Chiraz Larbi Aguili, and Taoufik Aguili. The renormalization group theory combined to the ms-gec method to study active fractal structures with incorporated pin diodes. *Progress In Electromagnetics Research*, 29:43–62, 2011.

[70] Houssemeddine Krraoui and Taoufik Aguili. Application of generalized equivalent circuits (gec) method for calculating of the diffraction by dielectric obstacles with finite thickness in metallic waveguide: application to the characterization of vegetation leaves. In *2014 Loughborough Antennas and Propagation Conference (LAPC)*, pages 617–621. IEEE, 2014.

[71] Messaoudi Hafawa. *Modélisation Électromagnétique du Phénomène d'Interaction des Ondes GSM avec la Tête Humaine par la Méthode des Circuits Équivalents Généralisés (MoM-GEC) dans un milieu fermé.* PhD thesis, Ecole Nationale d'Ingénieurs de Tunis, 2017.

[72] H Baudrand and D Bajon. Equivalent circuit representation for integral formulations of electromagnetic problems. *International Journal of Numerical Modelling: Electronic Networks, Devices and Fields*, 15(1):23–57, 2002.

[73] Bilel Hamdi. Modelisation des circuits periodiques et quasi-periodiques alimentes par des sources arbitraires. 2015.

[74] Abdessalem Kaddouri, Mourad Aidi, and Taoufik Aguili. A new approach based on mom-gec method to mutual coupling analysis of symmetric twin waveguides for antenna applications. *Journal of Electromagnetic Analysis and Applications*, 7(12):283, 2015.

[75] Mourad Aidi, Mohamed Hajji, Bilel Hamdi, and Taoufik Aguili. Graphene nanoribbon modeling based on mom-gec method for antenna applications in the terahertz range. In *2015 World Symposium on Mechatronics Engineering & Applied Physics (WSMEAP)*, pages 1–4. IEEE, 2015.

[76] Ahmed Nouainia, Bilel Hamdi, and Taoufik Aguili. Waveguide shielding analysis of 1d and 2d planar rectangular metallic structures using modified mom-gec method based on wave concept. *Radiation Physics and Chemistry*, 150:189–198, 2018.

[77] Lawrence Patrick Dunleavy. Discontinuity characterization in shielded microstrip: A theoretical and experimental study. 1988.

[78] Lawrence P Dunleavy and Pisti B Katehi. A generalized method for analyzing shielded thin microstrip discontinuities. *IEEE transactions on microwave theory and techniques*, 36(12):1758–1766, 1988.

[79] Robert W Jackson and David M Pozar. Full-wave analysis of microstrip open-end and gap discontinuities. *IEEE transactions on microwave theory and techniques*, 33(10):1036–1042, 1985.

[80] T Aguili, K Grayaa, A Bouallegue, and H Baudrand. Application of a source method for modelling step discontinuities in microstrip circuit. *IEE Proceedings-Microwaves, Antennas and Propagation*, 143(2):169–173, 1996.

[81] Raje Mchaalia, Mourad Aidi, and Taoufik Aguili. Study of planar structure applying reciprocity technique combined with mgec and analysis of discontinuity. *International Journal of RF and Microwave Computer-Aided Engineering*, page e21856.

[82] Cem Cansever. Design of a microstrip bandpass filter for 3.1-10.6 ghz uwb systems. 2013.

[83] Vivek Singh Kushwah, Geetam Singh Tomar, and Sarita Singh Bhadauria. Design of grooved microstrip patch resonator filters for mobile communication. *International Journal of Future Generation Communication and Networking*, 9(5):131–142, 2016.

[84] Arjun Kumar and MV Kartikeyan. Design and realization of microstrip filters with new defected ground structure (dgs). *Engineering Science and Technology, an International Journal*, 20(2):679–686, 2017.

[85] V Easwaran, VH Gupta, and ML Munjal. Relationship between the impedance matrix and the transfer matrix with specific reference to symmetrical, reciprocal and conservative systems. *Journal of Sound and Vibration*, 161(3):515–525, 1993.